Photochemical Formation of the Anion Radical of Zinc Phthalocyanine and Analysis of the Absorption and Magnetic Circular Dichroism Spectral Data. Assignment of the Optical Spectrum of [ZnPc(−3)]⁻

John Mack and Martin J. Stillman*

Contribution from the Department of Chemistry, University of Western Ontario, London, Ontario, Canada N6A 5B7

Received July 21, 1993®

Abstract: An extensive analysis of the optical absorption and magnetic circular dichroism (MCD) spectra of the anion radical of zinc phthalocyanine ([(ZnPc(−3)]⁻) is described. Novel photochemical formation of the ring-reduced [ZnPc(−3)]⁻ from (hydrazine)Zn^{II}Pc(−2) is reported for reactions carried out at room temperature using visible-wavelength light and hydrazine as the electron donor. Absorption and MCD spectra of the radical anion species have been obtained at both room and cryogenic temperatures. Phosphorescence and fluorescence lifetime studies of ZnPc(−2) show that the photoexcited (hydrazine)ZnPc(−2) complex reacts via the triplet state to form the ring reduced anion radical, [ZnPc(−3)]⁻. The complete lack of temperature dependence assignable to orbital degeneracies in the low-temperature MCD spectrum shows conclusively that the ^2E_g ground state of [ZnPc(−3)]⁻ is split into nondegenerate components at least 800 cm⁻¹ apart. The ground and excited states are completely nondegenerate. It is proposed that the coupled effects of the loss of aromaticity with the addition of the 19th π-electron, Jahn–Teller distortion, and nonsymmetric solvation of the ring lead to a change in molecular geometry from D_{4h} of ZnPc(−2) to C_{2v} for [ZnPc(−3)]⁻. The first complete assignment of the optical spectrum of any porphyrin or phthalocyanine anion radical is proposed on the basis of a $^2B_1$ ground state and supported by results from extensive deconvolution calculations. Comparison between the absorption and MCD spectral data indicated that a significant fraction of the spectral intensity observed at room temperature can be assigned as "hot" bands. The hot bands, which are much more pronounced in the spectral data of [ZnPc(−3)]⁻ than in the spectral data of the parent ZnPc(−2), are associated with interactions between the solvent, the Pc(−3) ring, and vibronic bands associated with the split ground state. A detailed study of the temperature dependence of the absorption and MCD spectra showed that meaningful spectral deconvolution calculations could only be carried out on spectra obtained from vitrified solutions of [ZnPc(−3)]⁻ at cryogenic temperatures. Bandwidths calculated to fit the absorption spectrum increase in magnitude as a function of the transition energy from 10 000 to 33 000 cm⁻¹, which allows the classification of sets of bands to one of five major electronic transitions, namely, Q between 750 and 1000 nm, n → π* between 580 and 750 nm, π* → π* between 430 and 650 nm, B1 and B2 between 300 and 450 nm.

Introduction

The aromatic π-system in the phthalocyanines and porphyrins results in a rich chemistry.[1-10] Metalation of these rings leads to complexes with a new ligand chemistry at the metal center and redox properties at both the metal and the ring. Figure 1 shows the molecular geometry of zinc phthalocyanine, ZnPc(−2). Although the aromatic ring itself is planar, the zinc is displaced 48 pm from this plane, with Zn–N bond lengths of 206.1 pm, to form a domed shape.[2] As transitions associated with the planar phthalocyanine ligand completely dominate the UV–visible absorption spectrum, D_{4h} symmetry has been assumed in previous spectral studies.[3] ZnPc(−2) is a useful model compound for studying the transition metal phthalocyanine and porphyrin complexes where charge transfer between the metal and ring can lead to very complex optical spectra.[3]

Redox reactions of the ring are an important chemical property of both synthetic and natural porphyrins.[4] Ring oxidation of the phthalocyanines and porphyrins to the π radical cation MPc(−1) or MP(−1) is well-known,[1,3-8] and optical spectra have been reported for many different species. Ring oxidation is a key component of the reaction mechanism proposed for the catalatic and peroxidatic reactions of the naturally occurring hemes in the

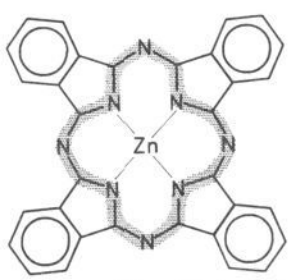

Figure 1. Molecular structure of zinc phthalocyanine showing the path of the 16-membered cyclic polyene ring that forms the basis for the four-orbital calculations of Gouterman used to account for the two lowest energy transitions in porphyrins and phthalocyanines.[18]

* To whom correspondence should be addressed. Fax: (519) 661-3022. Tel: (519) 661-3821. INTERNET: Stillman@uwo.ca.

® Abstract published in *Advance ACS Abstracts,* January 1, 1994.

(1) (a) *Phthalocyanine. Principles and Properties*; Lever, A. B. P., Leznoff, C. C., Eds.; VCH Publications: New York, 1989; Part I. (b) *Phthalocyanine. Principles and Properties*; Lever, A. B. P., Leznoff, C. C., Eds.; VCH Publications: New York, 1993; Part III.

(2) Kobayashi, T.; Ashida, T.; Uyeda, N.; Surro, E.; Kakuda, M. *Bull. Chem. Soc. Jpn.* **1971**, *44*, 2095.

(3) (a) Stillman, M. J.; Nyokong, T. N. In *Phthalocyanine. Principles and Properties*; Lever, A. B. P., Leznoff, C. C., Eds.; VCH Publications: New York, 1989; Part I, Chapter 3, pp 133–289. (b) Stillman, M. J. In *Phthalocyanine. Principles and Properties*; Lever, A. B. P., Leznoff, C. C., Eds.; VCH Publications: New York, 1993; Part III, Chapter 5, pp 227–296.

(4) (a) *The Porphyrins*; Dolphin, D., Ed.; Academic Press: New York, 1978. (b) Dolphin, D. *Ann. N.Y. Acad. Sci.* **1973**, 206.

(5) (a) Suslick, K. S.; Watson, R. A. *New J. Chem.* **1992**, *16*, 633. (b) Homborg, H.; Kalz, W. *Z. Naturforsch.* **1978**, *33B*, 1067.

(6) (a) Nyokong, T.; Gasyna, Z.; Stillman, M. J. *Inorg. Chem.* **1987**, *26*, 548. (b) Nyokong, T.; Gasyna, Z.; Stillman, M. J. *Inorg. Chem.* **1987**, *26*, 1087.

(7) (a) Ough, E. A.; Nyokong, T.; Creber, K. A. M.; Stillman, M. J. *Inorg. Chem.* **1988**, *27*, 2724. (b) Ough, E. A.; Gasyna, Z.; Stillman, M. J. *Inorg. Chem.* **1991**, *30*, 2301. (c) Ough, E. A.; Stillman, M. J. *Inorg. Chem.* **1994**, *33*, 573.

0002-7863/94/1516-1292$04.50/0

catalase and peroxidase enzymes.[9] There is considerable current interest in the chemical and spectral properties of the ring-reduced anion radical species of metal porphyrin and phthalocyanine (Pc) complexes.[10] A number of groups have studied the reduction of synthetic Ni porphyrins[11] as models of coenzyme F430, a nickel-containing tetrapyrrole that is involved in the reductive cleavage of *S*-methyl coenzyme to coenzyme M and methane. Reduction of both porphyrins and phthalocyanines has been reported,[10-17] and some spectral data have been described; however, no complete assignment of the optical spectra of these anion radical species has appeared to date. Because the lowest energy singlet band in the phthalocyanines is well separated from all other bands, metallophthalocyanines offer an ideal model system from which to build an assignment. Lever and co-workers have reported UV–visible absorption spectra for the anion and dianion radicals of the perchlorinated phthalocyanines of Fe, Co, and Zn.[17] Considerable industrial research into the properties of these compounds has been carried out. Possible uses as optical recording medium substrates, infrared light detectors, and reprographic photoreceptors have been envisaged.[17] With the exception of a preliminary report from this laboratory,[13] no recent MCD spectra have been reported for either ring-reduced phthalocyanines or ring-reduced porphyrins.

While spectroscopic analysis of the radical cations identifies low-lying filled molecular orbitals (MOs) as a result of the new $\pi \rightarrow \pi$ transitions *into* the partially filled highest occupied MO (HOMO),[3b,5-9] analysis of the radical anion spectra will lead to identification of the more energetic antibonding, unoccupied MOs through $\pi^* \rightarrow \pi^*$ transitions *from* the lowest unoccupied MO (LUMO) into MOs not normally accessible optically. Although many theoretical calculations have reported energies of the π and π^* molecular orbitals in porphyrins and phthalocyanines,[18-21] it has been difficult to verify the energies of the higher lying π^* orbitals because transitions in neutral MP(-2) and MPc(-2) complexes lie to the blue of 250 nm. Occupation of the e_g π^* orbital in the radical anion offers access to these high-lying π^* orbitals with transition energies that should lie in the UV–visible region. Analysis of the resonance Raman data[22] for the radical anion of zinc octaethylporphyrin, [ZnOEP(-3)]$^-$, suggested that the ground state was only slightly distorted by Jahn–Teller interactions from the D_{4h} symmetry of the neutral. In contrast, the distortion of the ground state of the anion radical of zinc tetraphenylporphyrin, [ZnTPP(-3)]$^-$, was much more significant.[22] The MCD experiment provides the information that is required to confirm unambiguously the ground- and excited-state degeneracies predicted from the Raman data.

MCD spectroscopy is complementary to UV–visible absorption spectroscopy in providing information about ground- and excited-state degeneracies that is essential in understanding the electronic structure of molecules of high symmetry.[3,23] The specificity of the MCD technique arises from three highly characteristic spectral features, the Faraday *A*, *B*, and *C* terms.[24] The derivative-shaped *A* term is temperature independent and identifies degenerate excited states, while the Gaussian-shaped *C* term is highly temperature dependent and identifies an orbitally degenerate ground state. Although not normally of as much utility in the assignment of the spectral data of symmetric molecules, the signs of the Gaussian-shaped temperature-independent *B* terms that arise from mixing between closely related states with *x*- or *y*-polarization can provide definitive data on the symmetry of excited states.[24] In this paper, spectral deconvolution of the extensively overlapped UV–visible absorption and MCD spectra of [ZnPc(-3)]$^-$ recorded at cryogenic temperatures are used to assign for the first time the major transitions in the spectrum of the radical anion between 1000 nm (10 000 cm^{-1}) and 290 nm (34 000 cm^{-1}).

Previous spectroscopic studies of the radical anions of metallophthalocyanines (MPc) have typically been based on spectroelectrochemistry[3b,13,15] or chemical reduction using sodium films in evacuated flasks.[12,14,16] The high reactivities of these paramagnetic anion radicals toward oxygen make the experimental procedures involved in studies of their spectral properties difficult. Progress in understanding the electronic structure of metallophthalocyanine radical anion species has therefore been hampered by a lack of spectral data of a sufficiently high quality for detailed analysis. We report in this paper the measurement and analysis of the absorption and MCD spectra of the radical anion species of ZnPc formed photochemically at room and cryogenic temperatures in absorption and MCD spectroscopic cuvettes.

Experimental Section

ZnPc (Eastman Kodak) and all solvents (Spectrograde) were used as received. ZnPc was analyzed by mass spectrometry and gave the expected

(8) (a) Gasyna, Z.; Stillman, M. J. *Inorg. Chem.* **1990**, *29*, 5101. (b) Nyokong, T.; Gasyna, Z.; Stillman, M. J. *ACS Symp. Ser.* **1986**, *321*, 309. (c) Gasyna, Z.; Browett, W. R.; Stillman, M. J. *ACS Symp. Ser.* **1986**, *321*, 298. (d) Gasyna, Z.; Browett, W. R.; Stillman, M. J. *Inorg. Chem.* **1984**, *23*, 382. (e) Gasyna, Z.; Browett, W. R.; Stillman, M. J. *Inorg. Chem.* **1985**, *24*, 2440.

(9) (a) Browett, W. R.; Gasyna, Z.; Stillman, M. J. *J. Am. Chem. Soc.* **1988**, *110*, 3633. (b) Gasyna, Z.; Browett, W. R.; Stillman, M. J. *Biochemistry* **1988**, *27*, 2503. (c) Browett, W. R.; Stillman, M. J. *Biochim. Biophys. Acta* **1981**, *660*, 1. (d) Browett, W. R.; Stillman, M. J. *Biochim. Biophys. Acta* **1980**, *623*, 21. (e) Dolphin, D.; Forman, A.; Borg, D. C.; Fajer, J.; Felton, R. H. *Proc. Natl. Acad. Sci. U.S.A.* **1971**, *68*, 614.

(10) (a) Yamaguchi, K.; Morishima, I. *Inorg. Chem.* **1992**, *31*, 3216. (b) Lever, A. B. P.; Wilshire, J. P. *Inorg. Chem.* **1978**, *17*, 1145. (c) Cosma, R.; Kautz, C.; Meerholz, K.; Heinze, J.; Mullen, K. *Angew. Chem. (Int. Ed. Engl.)* **1989**, *28*, 604. (d) Richoux, M. C.; Neta, P.; Harriman, A.; Baral, S.; Hambright, P. *J. Phys. Chem.* **1986**, *90*, 2462. (e) Kadish, K. M.; Liu, Y. H.; Sazou, D.; Sengler, N.; Guilard, R. *Anal. Chim. Acta* **1991**, *251*, 47. (f) Bottomley, L. A.; Chiou, W. J. H. *J. Electroanal. Chem. Interfacial Electrochem.* **1986**, *198*, 331. (g) Mosseri, S.; Nahor, G. S.; Neta, P.; Hambright, P. *J. Chem. Soc., Faraday Trans.* **1991**, *87*, 2567.

(11) (a) Kadish, K. M.; Sazou, D.; Liu, Y. M.; Saoiabi, A.; Ferhat, M.; Guilard, R. *Inorg. Chem.* **1988**, *27*, 1198. (b) Stolzenberg, A. M.; Stershic, M. T. *J. Am. Chem. Soc.* **1988**, *110*, 6391. (c) Lexa, D.; Momenteau, M.; Mispelter, J.; Saveant, J.-M. *Inorg. Chem.* **1989**, *28*, 30. (d) Nahor, G. S.; Neta, P.; Hambright, P.; Robinson, L. R.; Harrisman, A. *J. Phys. Chem.* **1990**, *94*, 6659. (e) Renner, M. W.; Furenlid, L. R.; Barkigia, K. M.; Forman, A.; Shim, H.-K.; Simpson, D. J.; Smith, K. M.; Fajer, J. *J. Am. Chem. Soc.* **1991**, *113*, 6891. (f) Stolzenburg, A. M.; Schussel, L. J. *Inorg. Chem.* **1991**, *30*, 3205. (g) Kadish, K. M.; Franzen, M. M.; Han, B. C.; Araullo-McAdams, C.; Sazou, D. *Inorg. Chem.* **1992**, *31*, 4399. (h) Helvenston, M. C.; Castro, C. E. *J. Am. Chem. Soc.* **1992**, *114*, 8490. (i) Procyk, A. D.; Stolzenberg, A. M.; Bocian, D. F. *Inorg. Chem.* **1993**, *32*, 627.

(12) (a) Clack, D. W.; Yandle, J. R. *Inorg. Chem.* **1972**, *11*, 1738. (b) Felton, R. H.; Linschitz, H. *J. Am. Chem. Soc.* **1966**, *88*, 1113.

(13) Mack, J.; Kirkby, S.; Ough, E. A.; Stillman, M. J. *Inorg. Chem.* **1992**, *31*, 1717.

(14) Dodd, J. W.; Hush, N. S. *J. Chem. Soc.* **1964**, 4607.

(15) Lindler, R. E.; Rowlands, J. R. *Mol. Phys.* **1971**, *21*, 417.

(16) Guzy, C. M.; Raynor, J. B.; Stodulski, L. P.; Symons, M. C. R. *J. Chem. Soc. A* **1969**, *10*, 997.

(17) Golovin, N. M.; Seymour, P.; Jayaraj, K.; Fu, Y.; Lever, A. B. P. *Inorg. Chem.* **1990**, *29*, 1719.

(18) Gouterman, M. In *The Porphyrins*; Dolphin, D., Ed.; Academic Press: New York, 1978; Vol. III, Part A, pp 1–165.

(19) Schaffer, A. M.; Gouterman, M.; Davidson, E. R. *Theor. Chim. Acta* **1973**, *30*, 9.

(20) McHugh, A. J.; Gouterman, M.; Weiss, C. *Theor. Chim. Acta* **1972**, *24*, 346.

(21) (a) Dedieu, A.; Rohmer, M.-M.; Veillard, A. *Adv. Quantum Chem.* **1982**, *16*, 43. (b) Orti, E.; Bredas, J. L.; Clarisse, C. *J. Chem. Phys.* **1990**, *92*, 1228. (c) Rosa, A.; Baerends, E. J. *Inorg. Chem.* **1992**, *31*, 4717. (d) Ishikawa, N.; Ohno, O.; Kaizu, Y.; Kobayashi, H. *J. Phys. Chem.* **1992**, *96*, 8832. (e) Ishikawa, N.; Ohno, O.; Kaizu, Y. *J. Phys. Chem.* **1993**, *97*, 1004. (f) Henriksson, A.; Roos, B.; Sundbom, M. *Theor. Chim. Acta* **1972**, *27*, 303.

(22) (a) Perng, J.-H.; Bocian, D. F. *J. Phys. Chem.* **1992**, *96*, 4804. (b) Reed, R. A.; Purrello, R.; Prendergast, K.; Spiro, T. G. *J. Phys. Chem.* **1991**, *95*, 9720.

(23) (a) Michl, J. *J. Am. Chem. Soc.* **1978**, *100*, 6801, 6812; *Pure Appl. Chem.* **1980**, *52*, 1549. (b) Waluk, J.; Muller, M.; Swiderek, P.; Kocher, M.; Vogel, E.; Hohlneicher, G.; Michl, J. *J. Am. Chem. Soc.* **1991**, *113*, 5511.

(24) (a) Piepho, S. B.; Schatz, P. N. *Group Theory in Spectroscopy with Applications to Magnetic Circular Dichroism*; Wiley: New York, 1983. (b) VanCott, T. C.; Rose, J. L.; Misener, G. C.; Williamson, B. E.; Schrimpf, A. E.; Boyle, M. E.; Schatz, P. N. *J. Phys. Chem.* **1989**, *93*, 2999. (c) Williamson, B. E.; VanCott, T. C.; Boyle, M. E.; Misener, G. C.; Stillman, M. J.; Schatz, P. N. *J. Am. Chem. Soc.* **1992**, *114*, 2412. (d) Stephens, P. J. *Adv. Chem. Phys.* **1976**, *35*, 197.

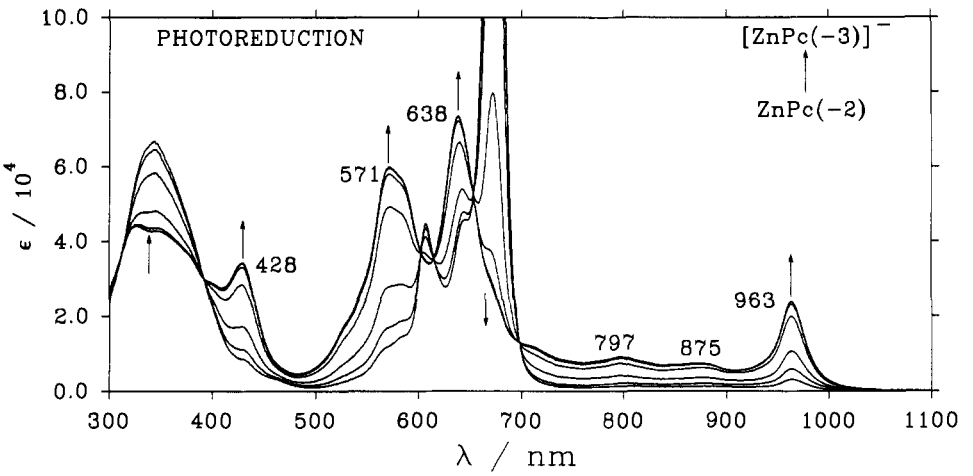

Figure 2. Absorption spectra recorded at room temperature during the photoreduction of a 10^{-5} M ZnPc(−2) in a 5/2 DMF/hydrazine hydrate solution. Excitation was restricted to wavelengths above 600 nm with a CS 2-73 Corning filter. Total elapsed time was 20 min. New bands are observed at 428, 571, 638, 797, 875, and 963 nm.

isotope patterns. Absorption spectra were recorded with an AVIV 17DS spectrophotometer (a spectrometer based on the Cary 17 monochromator). The room-temperature MCD spectra were obtained on the same solutions using a Jasco J500C spectrometer and a field of 5.5 T from an Oxford Instruments SM2 superconducting magnet. An SM4 magnet and a field of 4.0 T were used for cryogenic measurements. Spectra were recorded digitally under the control of an upgraded version of the program CDSCAN[25,26] running on an IBM 9000 series computer. The field strength and sign were calibrated by measuring the MCD spectrum of an aqueous solution of $CoSO_4$ at 510 nm. $[\theta]_M$ was calculated for this instrument to be −59.3° cm^2 dmol^{-1} T^{-1}. The signal intensity of the CD spectrometer was also tested using ammonium *d*-camphor-10-sulfonate by ensuring that the θ°/A ratio for the band at 280 nm was 2.26.[27] Electron paramagnetic resonance (EPR) measurements were made on a Bruker Model ESR 300 X-band spectrometer, at 20 K in an Oxford Instruments continuous-flow ESR 900 cryostat. EPR samples were prepared electrochemically and syphoned into 2 mm i.d. quartz EPR tubes which were then sealed under an inert atmosphere. An external DPPH standard was used to calculate *g* factors.

The room-temperature absorption and the fluorescence lifetimes were measured in a specially designed freeze–thaw emission cell. Solutions were degassed using standard freeze–thaw procedures. The solutions used for the room-temperature MCD spectra were prepared by siphoning deoxygenated solutions of ZnPc(−2) into evacuated cuvettes which were then sealed under an inert atmosphere with rubber septa. The photoreduction was carried out by excitation of the phthalocyanine Q band through irradiation with a 300-W tungsten–halogen Kodak projector lamp. A Corning CS 2-73 filter was used so that only light with wavelengths greater than 580 nm irradiated the sample. Low-temperature absorption spectra were measured, under a nitrogen atmosphere, in an Oxford Instruments Model CF-204 optical cryostat using the low-temperature spectroelectrochemical cells used in earlier cryogenic work on [MgPc(−3)]⁻.[13] Solutions were prepared at room temperature and cooled to −50 °C inside the CF-204 where photolysis was carried out on the liquid samples. The course of the photolysis was carefully monitored to ensure that the sample was quenched in liquid nitrogen to form a glass only after the reduction was complete. A specially designed spectroelectrochemical cell was used so that spectra could be measured on the same sample in both the CF-204 optical cryostat and the SM4 superconducting magnet.[13,28]

It is very difficult to obtain stable solutions of the highly reactive [ZnPc(−3)]⁻ anion radical even when the solution is degassed by the freeze–thaw technique. As the [ZnPc(−3)]⁻ anion also absorbs light throughout the 580–720-nm region it becomes progressively more difficult to photoreduce ZnPc(−2) as the reduction proceeds. Obtaining a solution in which 100% reduction has occurred to the radical anion species is therefore difficult. As a result, a minor impurity of ca. 1% ZnPc(−2) is invariably present in the room-temperature MCD spectra. Even when an impurity of only 2–3% is present, the very intense Q band of the ZnPc spectrum dominates the 650–690-nm region of the MCD spectrum. The spectral envelope of the ZnPc has been subtracted from the room-temperature spectra of the anion radical species shown in Figure 3. Baselines were subtracted from all the spectra reported. The spectral database program SPECTRA MANAGER was used in the manipulation of the data.[29] Deconvolution of the spectral data was carried out by using an upgraded version of the program SIMPFIT[30,31] on a Commodore Amiga 1000 computer.

Results and Discussion

Formation of the Radical Anion. As early as 1950, Evstigneev *et al.*[32] reported the photochemical formation of [MgPc(−3)]⁻ in pyridine solutions following exposure of MgPc(−2) to red light in the presence of ascorbic acid. de Backer *et al.*[33] used [MgPc(−3)]⁻ as an intermediate in the photochemical synthesis of dimethylhydrazine. Prolonged irradiation over several hours of a methylamine solution of MgPc in an evacuated quartz tube was required. Bobrovskii *et al.*[34,35] carried out photoreduction of MgPc at 215 K using anhydrous hydrazine in DMF. As MPc radical anions do not readily undergo hydrogen abstraction reactions, there is no reason that hydrazine hydrate (mp 216 K) cannot be used instead of anhydrous hydrazine (mp 276 K). The higher melting point of anhydrous hydrazine means that Bobrovskii *et al.* had to use very low concentrations to prevent vitrification of the solution at 215 K. This appears to have led to problems in carrying out the photochemical reduction to completion. Bobrovskii *et al.*[34,35] were also unable to produce suitable solutions for the measurement of spectra at cryogenic temperatures. In the study described here, the ring-reduced species, [ZnPc(−3)]⁻, was formed by photochemical reduction at both room temperature and −50 °C in a DMF/hydrazine hydrate solvent mixture which readily vitrifies to form transparent glasses.

Figure 2 shows absorption spectra measured at 298 K between 300 and 1100 nm during the photochemical reduction of ZnPc(−2) to [ZnPc(−3)]⁻ in 5/2 (v/v) DMF/hydrazine hydrate, using hydrazine as the electron donor. The set of spectra shown here exhibit extremely sharp isosbestic points with no indication of

(25) Gasyna, Z.; Browett, W. R.; Nyokong, T.; Kitchenham, R.; Stillman, M. J. *Chemom. Intell. Lab. Syst.* **1989**, *5*, 233.
(26) Mack, J.; Stillman, M. J. To be published.
(27) Chen, G. C.; Yang, J. T. *Anal. Lett.* **1977**, *10*, 1195.
(28) Radzki, S.; Mack, J.; Stillman, M. J. *New J. Chem.* **1992**, *16*, 583.
(29) Browett, W. R.; Stillman, M. J. *Comput. Chem.* **1987**, *11*, 73.
(30) Browett, W. R.; Stillman, M. J. *Comput. Chem.* **1987**, *11*, 241.
(31) Kirkby, S.; Mack, J.; Stillman, M. J. To be published.
(32) Evstigneev, V. B.; Gavrilova, V. A. *Dokl. Akad. Nauk SSSR* **1950**, *74*, 781.
(33) de Backer, M.; Jacquot, P.; Sauvage, F. X.; van Vlierberge, B.; Lepourte, G. *J. Chim. Phys.* **1987**, *84*, 429.
(34) Bobrovskii, A. P.; Maslov, V. G.; Sidorov, A. N.; Kholmogorov, V. E. *Dokl. Akad. Nauk SSSR* **1970**, *195*, 781.
(35) Bobrovskii, A. P.; Kholmogorov, V. E. *Russ. J. Phys. Chem.* (*Engl. Transl.*) **1973**, *47*, 983.

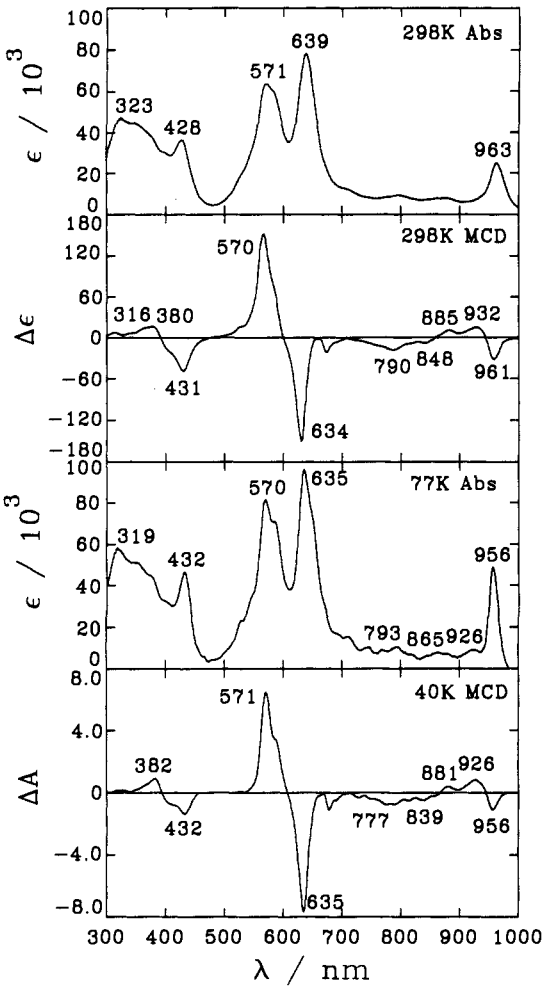

Figure 3. Absorption and MCD spectra of $[ZnPc(-3)]^-$ prepared photochemically at room temperature, recorded at 298 and 77 K. The absorption data show a general intensification, band narrowing, and blue shift at 77 K.

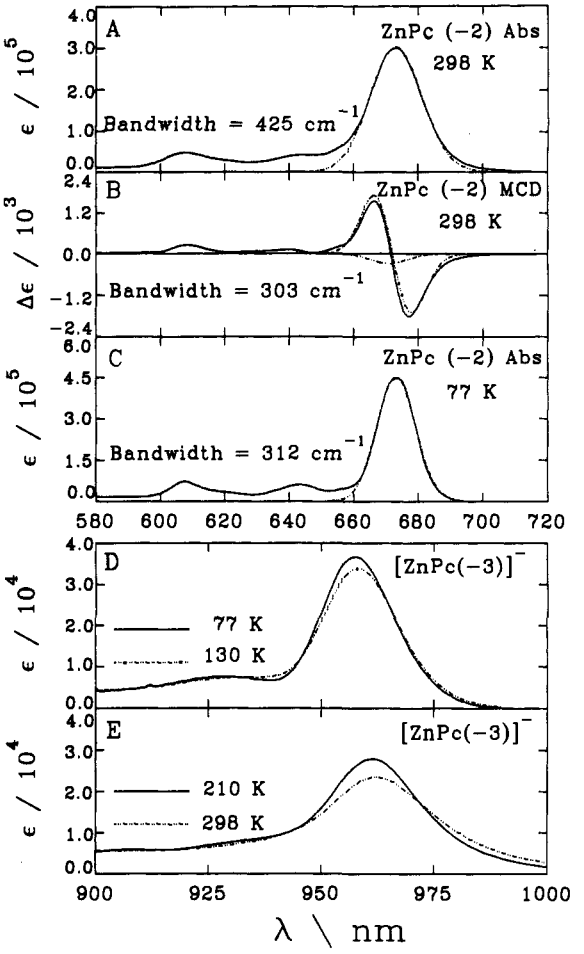

Figure 4. Comparison of the temperature dependence in the Q band region of the spectra of ZnPc(−2) and $[ZnPc(-3)]^-$. The Q band fits to a Guassian line shape with a bandwidth of 425 cm^{-1} (A); however, at room temperature the MCD envelope requires a much narrower bandwidth of 303 cm^{-1} (B). The absorption bandwidth matches the MCD bandwidth at 77 K (C). For $[ZnPc(-3)]^-$ the Q band at 960 nm both sharpens and blue-shifts between 298 and 77 K. The MCD band envelope aligns more exactly with the absorption spectrum recorded at 77 K (D).

decomposition or of secondary reaction products being formed. Care has to be taken in using the presence of isosbestic points as a criterion for purity, however. If the solution is insufficiently degassed or the solution is irradiated at excessively high light intensities, additional absorbance centered at 800 nm is observed, with the individual traces still connected by reasonably sharp isosbestic points in the 300–700-nm range. Only if the absorbance in the 700–1000-nm region changes consistently throughout the course of the reduction can the solution be used for detailed spectroscopic analysis. It should be noted that in none of the previous reports of the photochemical reduction of metallophthalocyanines were spectra included that were measured during the course of the reaction. The absorption spectra of $[MgPc(-3)]^-$ reported by Bobrovskii *et al.*[34,35] show a broad band at 800 nm that is consistent with the presence of a significant concentration of side reaction products. de Backer *et al.*[33] did not include this region of the spectrum in their report.

Figure 3 shows absorption and MCD spectra measured at 298 K (top) and 77 K (bottom). The absorption spectrum sharpens significantly at 77 K so that good estimates of the number and energies of the bands in the optical spectrum of the anion radical can be made. The major band centers are located at (using the 77 K spectrum) 319, 432, 570, 635, and 956 nm. Any residual parent ZnPc(−2) will exhibit a Q band (see below) at 670 nm. The Q band is the lowest energy transition of ZnPc(−2) and gives rise to an extremely intense *A* term in the MCD spectrum.[3a] Clearly, very little neutral ZnPc(−2) is present in the glass formed at 77 K. Similar band sharpening is observed for the parent ZnPc(−2) species between room temperature and 77 K (Figure 4A,B). Figure 3 shows that the major effect of the decrease in temperature is a general blue shift of the absorption band maxima in the spectra of $[ZnPc(-3)]^-$, especially at 639 and 963 nm. The effect can be seen clearly in Figure 4 where the spectral data for the Q band of ZnPc(−2) at 670 nm are compared with those for the Q band of $[ZnPc(-3)]^-$ that is centered on 960 nm (*vide infra*). This change in band characteristics signals the complexity of the states responsible for the absorption and MCD bands of $[ZnPc(-3)]^-$. This complexity is reflected in an unusual mismatch in the alignment between the major bands in the room-temperature absorption and MCD spectra in the 500–700- and 850–1050-nm regions (Figure 5). Using positively and negatively signed Gaussian line shapes, we illustrate how the MCD bands line up with only part of the absorption intensity at 298 K. The band shape of the absorption spectrum aligns much more closely with the MCD spectrum at low temperatures (see Figure 13). We will return to discuss this point in more detail below.

Figure 6 shows absorption and MCD spectra for the parent ZnPc(−2) in DMF at 298 K and the ring-reduced $[ZnPc(-3)]^-$ in DMF/hydrazine hydrate at 298 K on an energy scale. $[ZnPc(-3)]^-$ was formed photochemically as described in the Experimental Section. Unlike the spectrum of diamagnetic ZnPc(−2) complexes in which bands are localized in the 20 000–35 000-cm^{-1} (250–400-nm) and 14 000–17 000-cm^{-1} (600–700-nm) regions, the spectrum of the anion radical extends from 9500 to 35 000 cm^{-1} (250 to 1000 nm) with three prominent clusters of

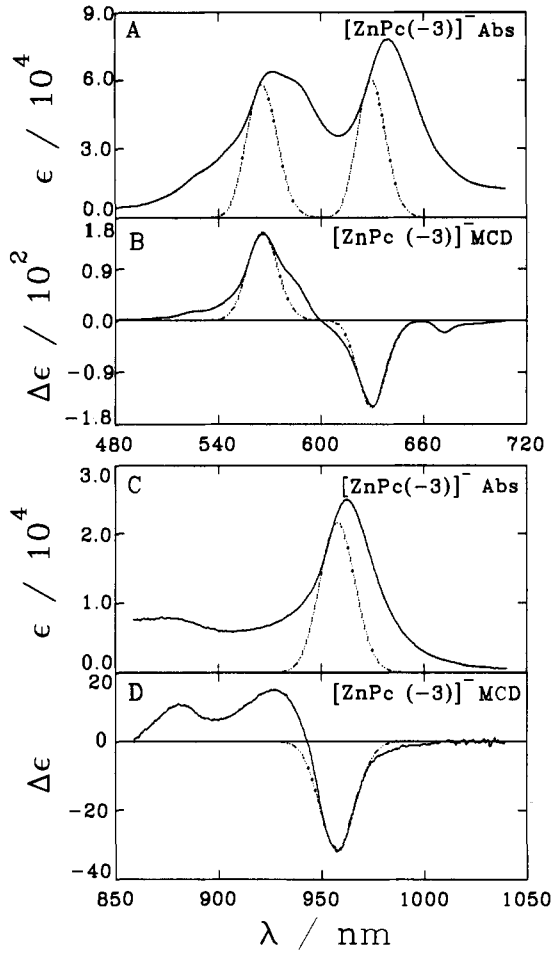

Figure 5. Room-temperature absorption and MCD spectra of the $\pi^* \rightarrow \pi^*$ transition region of $[ZnPc(-3)]^-$ (500–700 nm). Spectral bands are shown for the two major bands in the MCD spectrum. Bands with the same bandwidths and band centers are shown in the absorption spectrum showing the mismatch in band maximas between the absorption and MCD spectral envelopes.

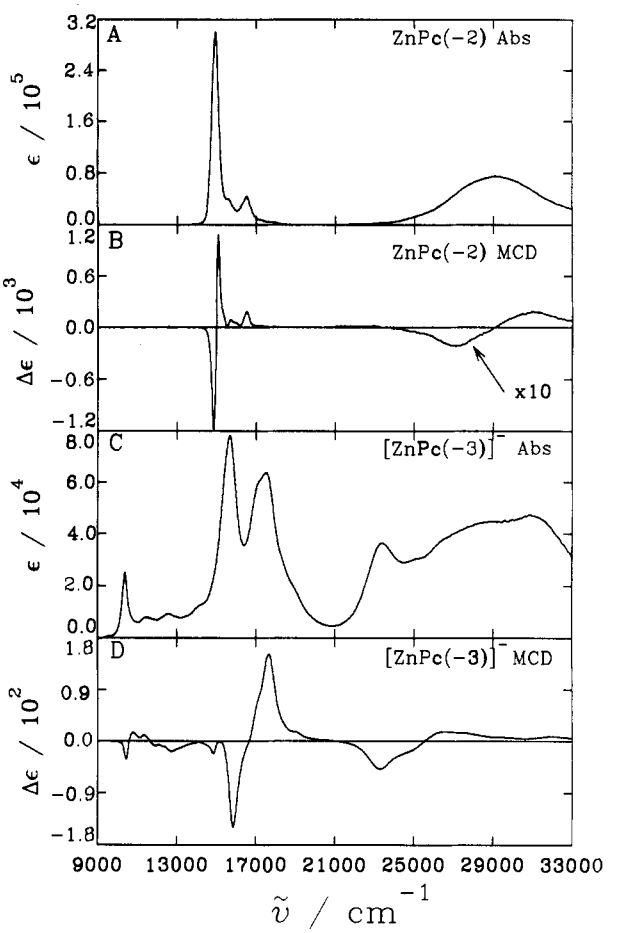

Figure 6. Absorption and MCD spectra for ZnPc(−2) in DMF (A, B) and $[ZnPc(-3)]^-$ in DMF/hydrazine hydrate (C, D). $[ZnPc(-3)]^-$ was prepared photochemically at room temperature as described in the experimental section. The abscissa is in energy units (cm^{-1}) to emphasize band-broadening effects for the set of bands at 960, 640, and 400 nm for $[ZnPc(-3)]^-$. The Q band of ZnPc(−2) lies near 14 000 cm^{-1} and the B1/B2 bands lie under the broad band at 29 000 cm^{-1}. The positive *A* term identifies the degeneracy of the lowest energy S_1 state; both B1 and B2 can be fit with *A* terms.[6] The Q band of $[ZnPc(-3)]^-$ is located near 10 400 cm^{-1}. None of the MCD bands observed for $[ZnPc(-3)]^-$ can be fit with *A* terms.

bands, centered on 10 420, 16 670, and 25 000 cm^{-1} (960, 600, and 400 nm). The MCD spectrum shows recurring coupled pairs of bands (negatively-signed to low energy and positively-signed to high energy of the crossover point) in each of these regions that show no significant temperature dependence.[13] These pairs of oppositely-signed *B* terms are observed at 10 440/10 810 cm^{-1} [958(±)/925(−) nm], 15 730/17 550 cm^{-1} [635(−)/569(+) nm], and 23 030/26 090 cm^{-1} [434(−)/383(+) nm] in the MCD spectrum measured at 40 K (Figure 3). As each of these coupled pairs of *B* terms correspond to two separate peaks in the absorption spectrum, it is safe to conclude that there are no *A* or *C* terms in the MCD spectrum. This is unambiguous evidence for a complete lifting of ground- and excited-state degeneracies. A number of key features are apparent. The alternating −/+ signs of the *B* terms that comprise the MCD envelope in the three spectral regions of the anion radical are the same as the sign alternation of the *A* terms in the parent ZnPc(−2) [see refs 3, 6, and 7 for descriptions of the deconvolution of the absorption and MCD spectra of MgPc(−2) and ZnPc(−2)]. This behavior is typical of *x*- and *y*-polarized transitions to close-lying, coupled excited states, and the MCD spectral effect has been termed a "pseudo *A* term".[24a,d] *These MCD spectral features, and especially the band at 10 440 cm^{-1} (958 nm)*, are characteristic marker bands for ring-reduced phthalocyanine radical anions.[12a]

Photochemical Mechanism. In the photoassisted reduction used here, hydrazine is employed as the electron donor, in much the same way as that we used CBr_4 as an electron acceptor in the ring oxidations of MPc(−2) to MPc(−1).[8] Hydrazine is a powerful reducing agent. The addition of hydrazine to solutions of Co^{II}Pc(−2) and Mn^{II}Pc(−2) causes reduction at the metal centers in the absence of light.[36] Hydrazine, however, cannot directly reduce the ground-state singlet phthalocyanine ring. The redox couple ZnPc(−2)/ZnPc(−3) potential is reported to be −0.97 V.[6a] The redox potentials of $N_2H_4/N_2H_4^+$ and the corresponding reaction of hydrazine hydrate were calculated to be −0.24 V at a platinum electrode in dimethyl sulfoxide.[37] However, in the triplet excited state, the redox couple ZnPc(−2)/ZnPc(−3) is greatly modified so that ring reduction occurs with a potential of +0.71 V.[38] As a result, the reduction of the phthalocyanine ring becomes thermodynamically favored in the presence of hydrazine. All the potentials quoted are relative to the saturated calomel electrode.

Photoreduction of ZnPc(−2) takes place readily in the presence of hydrazine at room temperature even when a filter (Corning 2-73) that absorbs light of wavelengths shorter than 580 nm is used. This indicates that the charge transfer takes place through either the S_1 or the T_1 state of the phthalocyanine ring, as neither

(36) Mack, J.; Stillman, M. J. Unpublished.
(37) Michylmayer, M.; Sawyer, D. T. *J. Electroanal. Chem. Interfacial Electrochem.* **1969**, *23*, 375.
(38) Ferraudi, G. In *Phthalocyanine. Principles and Properties*; Lever, A. B. P., Leznoff, C. C., Eds.; VCH Publications: New York, 1989; Part I, Chapter 4, pp 291–340.

Table 1. Band Centers of the Q_{00} Band of 10^{-5} M ZnPc(−2) on Addition of Hydrazine

concn (M)	band center (nm)	concn (M)	band center (nm)
0	669.0	10^{-4}	670.6
10^{-7}	668.9	10^{-1}	670.8

hydrazine nor hydrazine hydrate absorb in the visible region. The electron-transfer reactions of the lowest lying photoexcited triplet and singlet states of MPc complexes have been studied by a number of groups.[38-46] Flash photolysis studies[46] have shown that both cation and anion radical species can be formed through quenching reactions of the excited triplet state of metallophthalocyanines. The quenching process leads to the formation of a geminate radical pair. The reaction then proceeds either through reverse electron transfer to the original ground state or through dissociation of the electron acceptor and donor to form the products.[6,8,46] The paramagnetic anion radical is a highly reactive species and, therefore, can undergo a number of side reactions. To minimize these reactions, polar aprotic solvents were used and the photoreduction was carried out under an inert atmosphere.

Most photochemical reactions that have been studied exhibit bimolecular mechanisms that depend upon collisions between the photoexcited phthalocyanine and the donor or acceptor molecule.[46] Absorption profiles and excited-state measurements can be used to detect the presence of axial ligands. The addition of hydrazine at concentrations that are at least equimolar with the 10^{-5} M solution of ZnPc in DMF causes a sharp shift in the wavelength of the maximum of the Q-band absorbance (Table 1). The band maximum does not shift significantly at higher concentrations, indicating that the band shift is due to direct ligation of the metal by the hydrazine. Clearly, (hydrazine)-ZnPc(−2) is the form of the irradiated complex, with charge transfer taking place through the excited state of the ring. As the hydrazine is bound to the ZnPc(−2), the reaction is very efficient.

Although reduction normally occurs via the lowest lying excited triplet state, a number of metalloporphyrin complexes can also be reduced via the lowest lying excited singlet state.[41] Charge transfer that is initiated from an excited state can be determined by examining quenching of the excited-state lifetime. Both fluorescence and phosphorescence spectra can be measured for ZnPc and ZnP, where P represents a number of different porphyrins.[8,46] However, the phosphorescence spectra of ZnPc and MgPc are centered near 1100 nm,[38] which lies outside the range that is easily detectable using conventional emission spectrometers. By comparison with the excited-state properties observed for the photoreduction of zinc tetraphenylporphyrin (ZnTPP), we can show that the reduction must occur via the lowest lying triplet excited state of the ZnPc(−2) complex. The fluorescence decay curves for the lowest lying excited singlet states of ZnPc and ZnTPP yield lifetimes of 4.3 ± 0.8 ns at 690 nm for ZnPc and 1.6 ± 0.3 ns at 622 nm for ZnTPP. These lifetimes are relatively unaffected by the addition of hydrazine to the solutions; ZnPc + hydrazine, 4.3 ± 0.8 ns; ZnTPP + hydrazine, 1.8 ± 0.3 ns. On the other hand, the lifetime of the triplet state of ZnTPP(−2) is much shorter in the presence of hydrazine (at ca. 24 ms in the absence of hydrazine vs ca. 12 ms with hydrazine).[47] We can summarize the reaction for the formation of the radical anion as

$$\text{(hydrazine)ZnPc(}-2\text{)} \rightarrow \text{(hydrazine)ZnPc(}-2\text{)}^*;\ Q \text{ band excitation to } S_1 \text{ at 670 nm}$$

$$\rightarrow \text{(hydrazine)ZnPc(}-2\text{)}^*; \text{ intersystem crossing to } T_1$$

$$\rightarrow \text{(hydrazine)ZnPc(}-2\text{)}^*; \text{ activation of charge transfer and dissociation of bound oxidized hydrazine}$$

$$\rightarrow [\text{ZnPc}(-3)]^- + \text{hydrazine products (initially } N_2H_4^+\text{)}$$

Molecular Orbital Models Used for Spectral Analysis. (1) Neutral Porphyrins and Phthalocyanines, MP(−2) and MPc(−2). Several calculations have been reported that predict the energies of orbitals in metalloporphyrins and metallophthalocyanines, and in some instances assignments of the optical spectra of metallophthalocyanines have been made.[18-21,23] The spectral properties of the π-systems of both porphyrin- and phthalocyanine-ring complexes can initially be rationalized in terms of the cyclic polyene model.[18,23a] This simple model has served as the starting point from which to interpret the distinctive spectral properties of the porphyrins and phthalocyanines, in particular, the spectral features observed for the three most available species: the dianion, Pc(−2), the radical cation, Pc(−1), and the radical anion, Pc(−3). Bands in the 250–1000-nm range for $M^{II}Pc(-2)$ complexes in solution can be viewed as arising from a 16-atom, 18-π-electron, cyclic polyene aromatic system on the inner periphery of the phthalocyanine ring; see Figure 1. The π-system will be similar to that of benzene with a stack of seven degenerate orbitals of alternating ungerade and gerade parities with nondegenerate orbitals to low and high energy.[23a] The orbital angular momentum of the molecular orbitals of the aromatic ring, M_L, will increase in the sequence 0, ±1, ±2, etc. up the stack. The effect of the nitrogens in the pyrrole groups of the porphyrin skeleton is to lift the degeneracy of the ungerade molecular orbitals.[18]

The model that has been used most widely to describe the optical spectra of both the porphyrins and phthalocyanines are the calculations by Gouterman's group based on the PPP–LCAO–CI theoretical treatment.[18] A significant part of this work for spectroscopists has been the four-orbital approach in which the optical spectrum can be interpreted in terms of the a_{1u} and a_{2u} highest occupied molecular orbitals, the HOMOs, and the doubly degenerate e_g^* orbitals, the LUMO. In Gouterman's four-orbital approach,[20] transitions from the $M_L = \pm 4$ ground orbitals (a_{1u} and a_{2u}) to the $M_L = \pm 5$ orbitals (e_g) result in two states; the lower energy state is predicted to exhibit ±9 units of angular momentum (the Q band at 670 nm) while the upper state (B1 near 350 nm) will exhibit ±1 unit. This approach accounts well for the relative magnitude of the two major transitions seen in the UV–visible spectra of metal porphyrin complexes.[18]

Several effects are introduced by the aza nitrogens and fused benzene groups of the phthalocyanine. First, the presence of these groups further separates the components of the e_u molecular orbitals so that the top filled a_{1u} lies well above the a_{2u}

(39) Chernikov, V. S.; Poddubriaya, V. M.; Byteva, I. M. *Zh. Prikl. Spektrosk.* **1977**, *27*, 781.
(40) Poddubriaya, V. M.; Byteva, I. M.; Chernikov, V. S. *Biofizika* **1983**, *28*, 370.
(41) Darwent, J.; Douglas, P.; Harriman, A.; Porter, G.; Richoux, M. C. *Coord. Chem. Rev.* **1982**, *44*, 83.
(42) Darwent, J.; McCubbin, I.; Phillips, D. *J. Chem. Soc., Faraday Trans. 2* **1982**, *78*, 347.
(43) Prasad, D. R.; Ferraudi, G. *J. Phys. Chem.* **1982**, *86*, 4037.
(44) Prasad, D. R.; Ferraudi, G. *Inorg. Chem.* **1983**, *22*, 1672.
(45) Ferraudi, G.; Prasad, D. R. *J. Chem. Soc., Dalton Trans.* **1984**, 2137.
(46) Davidson, R. S. *Adv. Phys. Org. Chem.* **1983**, *19*, 1. .

(47) Excited-state lifetimes were recorded on a PTI LS100 instrument. Fluorescence lifetimes were measured at room temperature as follows: for ZnPc, excitation at 340 nm, emission monitored at 690 nm using a Corning CS 2-60 filter; for ZnTPP, excitation at 420 nm, emission monitored at 622 nm (no hydrazine) and 610 nm (in the presence of hydrazine) using a Corning CS 2-73 filter. 4-mL solutions in DMF were degassed in a freeze–thaw cycle, with 200 μL (ZnTPP) or 10 μL (ZnPc) of hydrazine hydrate added. The fluorescence decays were calculated by the software provided with the LS100 using a single-exponential fit. Phosphorescence lifetimes of ZnTPP in the absence and presence of hydrazine hydrate were measured in DMF/DMA (5/1) or DMF/DMA/hydrazine hydrate (5 mL/1 mL/10 μL) solutions, with excitation at 540 nm and the emission monitored at 780 nm. The gated phosphorescence was recorded with a boxcar integrator using 10-ms windows which were increased incrementally in 5-ms steps.

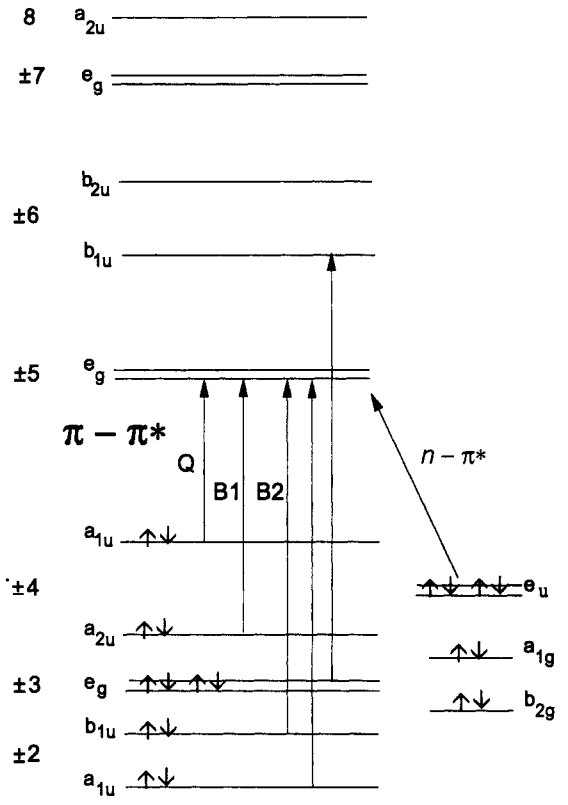

Figure 7. Molecular orbitals involved in the major $\pi \rightarrow \pi^*$ absorption transitions with energies between 10 000 and 35 000 cm^{-1} adapted from Schaffer, Gouterman, and Davidson.[19] The order of the orbitals is based on theoretical models for the ZnPc(–2) species.[6,7,24b] The Q, B1, and B2 transitions shown are those anticipated through application of Gouterman's four-orbital LCAO model[18,19] and from analysis of MCD data for ZnPc[6,24b] and MgPc.[7] The arrows indicate allowed transitions that give rise to bands observed in the 300–900-nm region of the absorption and MCD spectra. Each of the states generated will be degenerate, and MCD *A* terms are observed for each transition (ZnPc/MgPc). The association of orbital angular momentum with pairs of states follows from the assignment of the molecular orbitals of an aromatic ring in terms of orbital angular momentum in the sequence 0, ±1, ±2, etc. Note that the Q and B1 bands arise from transitions out of ±4 orbitals into ±5 orbitals and can be associated with an allowed ±1 transition (B1) and a "forbidden" ±9 transition (Q).[20]

component.[3a,18,21] The effect of this is to increase dramatically the requirement for intensity mixing between the lowest two singlet excited states, Q (S_1, at about 670 nm) and B1 (S_2, at about 340 nm), so that compared with that of many porphyrins, the energy of the Q band red-shifts to near 670 nm and dramatically intensifies to extinction coefficients of 10^5 L mol^{-1} cm^{-1}.[3a] In addition, unlike the situation with the porphyrins, two bands of similar intensity and bandwidths are observed in the 320-nm region, currently named B1 and B2.[3a,24b] Figure 7 illustrates the assignment of the three lowest energy transitions, Q, B1, and B2 (two further transitions are observed below 300 nm in the optical spectrum of diamagnetic phthalocyanines such as ZnPc(–2) and MgPc(–2)[6-8] and are named the N and L bands). Calculation of the energies and intensities of transitions in the optical absorption spectra of phthalocyanines indicates considerable mixing between the excited states,[21f] so the transitions shown in Figure 7 only represent a first-order assignment. None of the theoretical calculations that have been reported for even the neutral, diamagnetic phthalocyanines can completely account for the band energies, dipole strengths, and angular momentum properties of all five bands identified by deconvolution analysis of the MCD spectral data of MgPc(–2) and ZnPc(–2).[6,7] The basic orbital ordering reported by several groups does still coincide with that obtained from the cyclic polyene approach used for Figure 7.[19,21]

The most important recent technique with which to study the electronic states in the porphyrins and phthalocyanines is MCD spectroscopy because the MCD spectra are highly sensitive to the presence of orbital angular momenta.[23,24] Calculations of McHugh *et al.*[20] predict magnetic moments for the lowest two singlet states of MPc(–2) of –3.1 (Q band) and –0.63 (B1 band) in Bohr magnetons. Moments analysis of MCD data support these values.[3a,6] The ground states of divalent, main group metal phthalocyanine complexes with D_{4h} symmetry will be $^1A_{1g}$, and the accessible $\pi \rightarrow \pi^*$ excited states will be degenerate, ^1E_u (x/y-polarized). Vibronically coupled states can also transform as $^1A_{2u}$ (z-polarized). Transitions to the degenerate excited states will give Faraday *A* terms in the MCD spectrum, while the z-polarized vibrational bands will give Faraday *B* terms.

An additional complication in the case of metal phthalocyanine complexes is the presence of nonbonding orbitals on the aza nitrogen linkages. These orbitals would be expected to lie close to energy to the HOMO and LUMO of the cyclic polyene ring. As a result, $n \rightarrow \pi^*$ transitions can be expected to make a contribution to the optical spectrum.[19] Huang *et al.*[48] have shown that the fluorescence of the Q_{00} band measured in a Shpol'skii matrix at 4.2 K is not a mirror image of the corresponding excitation spectrum. These authors postulated that an $n \rightarrow \pi^*$ transition which couples with weak vibrational bands of the Q transition could be at least partly responsible for the 605-nm band seen to the blue of the main Q_{00} transition (Figure 4). Van Cott *et al.*[24b] later concluded that there may also be another $n \rightarrow \pi^*$ transition in the B region of the spectrum. While the $\pi \rightarrow \pi^*$ bands of the neutral ZnPc(–2) are extremely intense and will dominate weak bands, it is in the spectra of the cation and anion radicals that these $n \rightarrow \pi^*$ bands are most likely to be observed, as the $\pi \rightarrow \pi^*$ intensities are greatly diminished.[3b]

In summary, the spectrum of the neutral ZnPc(–2) (Figure 6) includes an intense Q band (ϵ ca. 10^5) near 670 nm, followed by a series of vibrational components, Q_{vib}. B1 and B2 are superimposed in the 350-nm region in the absence of strong axial ligands.[6,7] The N band lies near 270 nm.[6,7,24b] A significant feature in the spectrum of the phthalocyanines is that the bandwidths are considerably greater for the B1 and B2 bands than for the Q band and that the vibronic progression observed for the Q band is a complex superposition of a large number of component transitions; both of these effects can be understood in terms of the analysis of the spectra of large aromatic and heteroaromatic molecules described by Hochstrasser and Marzzacco.[49] On this basis, Schaffer *et al.*[19] proposed that the presence of an $n \rightarrow \pi^*$ transition at an energy lower than those of the B1 and B2 transitions could account for the significant broadening of these bands (Figure 6). The high-energy states (transitions to b_{1u}^* and b_{2u}^* and to orbitals with $M_L > \pm 6$) have not been completely assigned for the phthalocyanines because of band broadening in the vapor phase,[18] Davydov effects in thin films,[50] influence of solvent absorption below 230 nm,[3a] or multiple-site effects in matrix-isolated molecules.[24b,c]

(2) Ring-Reduced Anion Radicals, $[MPc(-3)]^-$. Ring reduction provides access to higher energy orbitals by placing an electron into the $M_L = \pm 5$ e_g^* orbital (Figure 8). Some of the now available $\pi^* \rightarrow \pi^*$ transitions will overlay the existing $\pi \rightarrow \pi^*$ transitions in the 250–1000-nm region. No recent molecular orbital calculations have been reported for the radical anions of either the porphyrins or the phthalocyanines. We expect the $\pi \rightarrow \pi^*$ and $n \rightarrow \pi^*$ transitions that are present in the optical spectrum of ZnPc(–2) will result in a similar set of bands in the $[ZnPc(-3)]^-$ spectrum but with different energies and with grossly

(48) (a) Huang, T. H.; Reickhoff, K. E.; Voight, E. M. *J. Chem. Phys.* **1982**, *77*, 3424. (b) Huang, T. H.; Reickhoff, K. E.; Voight, E. M. *J. Phys. Chem.* **1981**, *85*, 3322.
(49) Hochstrasser, R. M.; Marzzacco, C. *J. Chem. Phys.* **1968**, *49*, 971.
(50) (a) Hollebone, B. R.; Stillman, M. J. *J. Chem. Soc., Faraday Trans. 2* **1977**, *74*, 2107. (b) Hollebone, B. R.; Stillman, M. J. *Chem. Phys. Lett.* **1974**, *29*, 284.

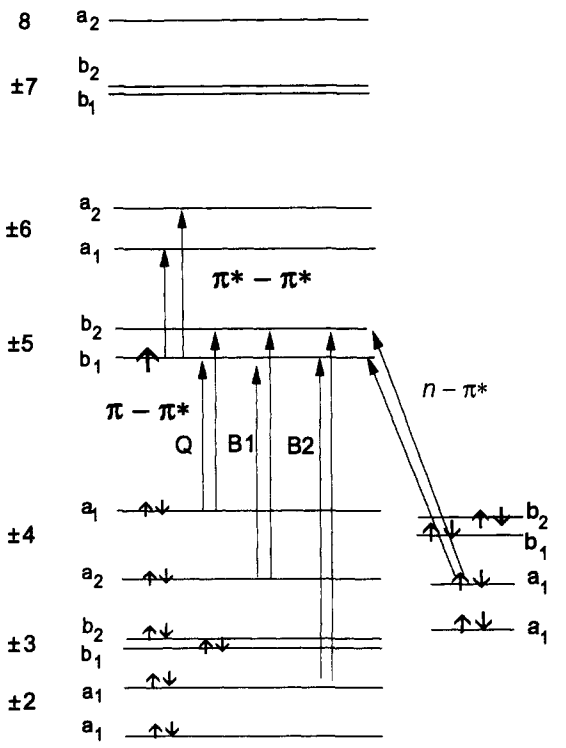

Figure 8. Molecular orbitals involved in the major $\pi \rightarrow \pi^*$ and $\pi^* \rightarrow \pi^*$ absorption transitions in the ring-reduced $[ZnPc(-3)]^-$ species with energies between 10 000 and 35 000 cm^{-1} adapted from Schaffer *et al.*[19] The order of the orbitals is based on theoretical models for the ZnPc(−2) and $[ZnPc(-3)]^-$ species.[21] No account has been taken of changes in the energies of the molecular orbitals as a result of different ring occupation upon reduction. The possible $\Delta M_L = \pm 1$ transitions are shown based on application of Gouterman's four-orbital LCAO model[18] as described for Figure 7. The $\pi \rightarrow \pi^*$ Q, B1, and B2 bands are expected to be less intense than for ZnPc(−2) due to changes that occur as a result of the partial occupation of the e_g^* orbital (in D_{4h} symmetry). New bands are expected for the transition out of the e_g^* orbital that is $\pi^* \rightarrow \pi^*$ in character. The orbitals shown are labeled for the proposed C_{2v} geometry and were obtained from the corresponding D_{4h} labeling through the use of correlation tables.

different intensities. The character of all the transitions that make up the optical spectrum of $[ZnPc(-3)]^-$ will depend entirely on the symmetry of the molecule.

Dimerization of the radical species of metal porphyrin and phthalocyanine complexes is to be expected at all temperatures.[7b] However, dimerization of phthalocyanines, both the neutral [MPc(−2)] compound and the radical cation $[MPc(-1)]^+$, exhibits the expected, strong temperature dependence:[3b] dimers are the preferred product at low temperatures; monomers, at room temperature and above. For the cation radical $[MgPc(-1)]^+$ species, we demonstrated clearly that this temperature dependence was associated with significant and characteristic changes in the absorption, and MCD, for spectra recorded over the 300–77 K range. No such changes were observed for the anion radical species, $[MgPc(-3)]^-$ [13] and $[ZnPc(-3)]^-$. Finally, dimerization would lead to a complete quenching of the EPR signal of the anion radical species of cryogenic temperatures. Typical derivative-shaped EPR signals were seen at $g = 2.0029 \pm 0.0004$ for $[MgPc(-3)]^-$ and $g = 2.0027 \pm 0.0004$ for $[ZnPc(-3)]^-$ at 20 K. The presence of the EPR signals confirm the doublet spin multiplicity and the lack of dimerization.

The observation that the MCD spectrum of $[ZnPc(-3)]^-$ is essentially temperature independent (Figure 3) unambiguously defines the ground state as nondegenerate. The anticipated ^2E_g ground state must split under the influence of Jahn–Teller effects and environmental effects introduced by solvation of the ring. There are two Jahn–Teller-active vibrations, with b_{1g} and b_{2g} symmetries, that could cause this zero-field orbital splitting.[51] The spectral properties of $[ZnPc(-3)]^-$ are determined by the magnitude of the ground-state splitting. If the distortion was small, two nearly degenerate ground states would be found, populated according to a Boltzmann distribution. Marked temperature dependence would be seen in the MCD spectrum at low temperatures as the population shifts to the lower orbital.[24a,d] The lack of significant temperature dependence in the MCD spectrum (Figure 3) therefore indicates that the zero-field orbital splitting of the ground state must be fairly substantial to ensure nearly 100% population of the lower state up to 298 K.

Figure 8 shows our proposed energy level diagram for phthalocyanine radical anion species and the allowed ring-based transitions based on C_{2v} symmetry. When an electron is added to the 18-π-electron system, the basic aromatic nature of the ring is lost as Huckel's rule is no longer obeyed. Ring planarity is therefore no longer energetically favored. The substantial zero-field orbital splitting of the ground state indicates that the ring must buckle under the influence of a static Jahn–Teller distortion and nonsymmetric solvation. X-ray crystallography studies on many metal porphyrin cation radicals, where the ring is also no longer aromatic, show that the ring buckles, with the pyrroles alternating above and below the plane of the ring, to adopt an approximate C_{2v} geometry.[52] A recent molecular mechanics study of metal porphyrin complexes showed that even aromatic rings associated with MP(−2) complexes are reasonably flexible.[53] Ruffling and doming can occur in response to the environment of the MP(−2) ring in biologically important proteins. Correlation tables were used to work out the appropriate labels for the orbitals under C_{2v} symmetry. The orbital and state diagrams predicted for the major transitions of $[ZnPc(-3)]^-$ are shown in Figures 8 and 15. Because the ground and excited states in $[ZnPc(-3)]^-$ are nondegenerate, all the x/y-polarized $\pi \rightarrow \pi^*$ transitions of ZnPc(−2) that were identified by positive A terms will be replaced by the coupled pairs of oppositely signed B terms.

Band Deconvolution Calculations. In previous papers from our group, spectral deconvolution calculations using the program SIMPFIT have been used as the basis for band assignments made for a variety of neutral and ring-oxidized metal phthalocyanine and porphyrin complexes.[3,6–8] The fitting procedures used are based upon the assumption that the bandwidths and band centers will be *identical* in both the absorption and MCD spectra if the rigid-shift approximation is made for the MCD spectral envelope.[24a,d] The rigid-shift assumption essentially implies that the band shape function is not affected by the applied magnetic field in the MCD experiment. This assumption is valid for transitions linking states that obey the Born–Oppenheimer approximation.[24a] The program SIMPFIT uses least-squares and Simplex iteration routines to obtain the best fit between calculated and experimental data by varying the band centers and bandwidths of the Gaussian-shaped bands that are assumed to make up the spectra. Holding the band parameters the same in both the absorption and MCD spectra introduces a "straitjacket" on the analysis that greatly reduces the ambiguity of the results. The assumption is made that the minimum number of bands should be used to fit the spectra, so that the removal of even one band results in a fit that is clearly unsatisfactory. Linking the absorption and MCD spectra ensures that the bands calculated are related to transitions of the molecule. The MCD spectrum provides the second data set that is required to make meaningful band deconvolution possible.[3,6–8]

The bandwidths seen for the Q_{00} band in the room-temperature absorption and MCD spectra for ZnPc(−2) in the Q band region clearly to not coincide (Figure 4). Sutherland[54] showed that, in

(51) (a) Minor, P. C.; Gouterman, M.; Lever, A. B. P. *Inorg. Chem.* **1985**, *24*, 1894. (b) Gouterman, M. *Ann. N.Y. Acad. Sci.* **1973**, *206*, 70.

(52) Gans, P.; Buisson, G.; Duee, E.; Marchon, J.-C.; Erler, B. S.; Scholz, W. F.; Reed, C. A. *J. Am. Chem. Soc.* **1986**, *108*, 1223.

(53) Munro. O. Q.; Bradley, J. C.; Hancock, R. D.; Marques, H. M.; Marsicano, F.; Wade, P. W. *J. Am. Chem. Soc.* **1992**, *114*, 7218.

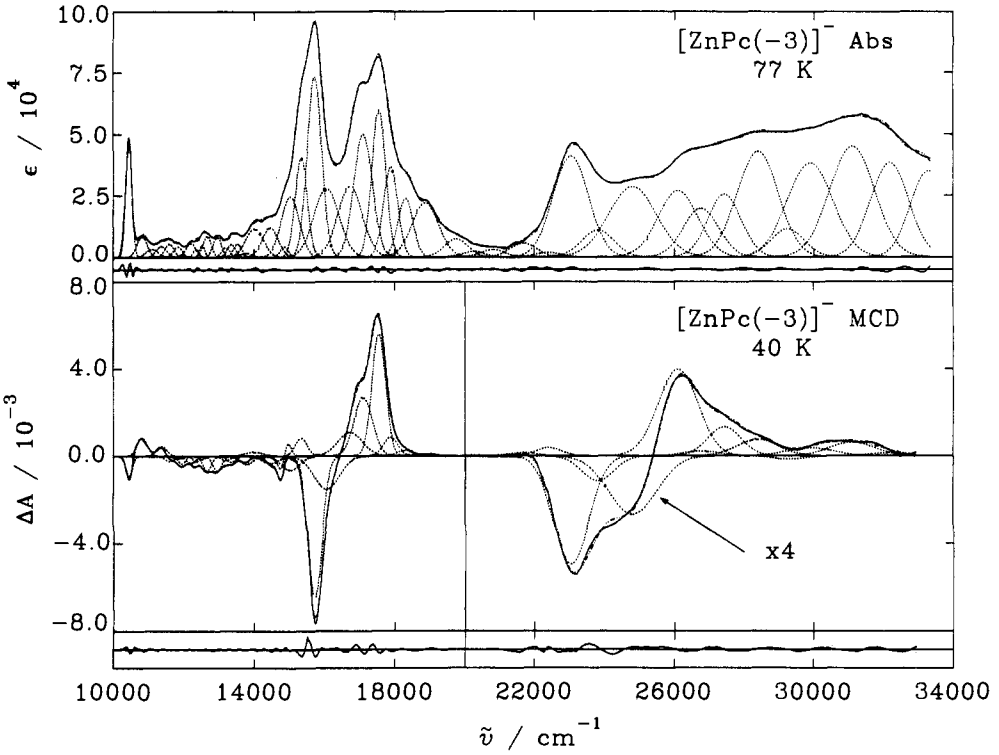

Figure 9. Complete set of 45 bands required to fill the absorption and MCD band envelopes of $[ZnPc(-3)]^-$. One additional band was required to account for the very intense Q_{00} band of ZnPc(−2). Only a very minor impurity of ZnPc(−2) is present (ca. 1%). The absorption spectrum was recorded at 77 K, and the MCD spectrum, at 40 K. The bands were fit using Gaussian components with the identical band centers and bandwidths for pairs of absorption and MCD bands. The bandwidths for the three regions (960, 640, and 400 nm) are clearly different. The weak, positive *A* term located at 14 860 cm^{-1} is due to residual neutral ZnPc(−2). The band parameters are summarized in Table 3.

an analogous situation with Zn(II) and Mg(II) coproporphyrin, zero-field orbital splitting of the excited state could account for this effect. Sutherland concluded that Jahn–Teller splitting in the Shpol'skii spectra of metalloporphyrins and metallophthalocyanines was too minor to account for the large discrepancy in the spectral bandwidths. He proposed that interaction between the ring and the surrounding solvent molecules was responsible for a reduction in the symmetry of the excited state. The multiplicity of possible environments led to a spread in the energy of the main transitions. As MCD spectroscopy depends upon the magnetic dipole moment in addition to the transition dipole moment, the intensity mechanism of MCD bands is significantly different from those seen in the absorption spectrum.[24a,d] Solvation environments which lead to a significant reduction in the overall symmetry will quench the angular momentum of the excited states in the wings of the MCD envelope resulting in a far sharper MCD band, (Figures 3–5). At cryogenic temperatures, however, the absorption band sharpens and intensifies and is almost perfectly Gaussian in shape. Figure 3 clearly shows that at 77 K, in contrast to the spectrum recorded at 298 K, the bandwidths of the Q band at 670 nm are similar in the absorption and MCD spectra, as the higher energy solvation environments are frozen out when the sample is vitrified.

Quantitative information can be obtained from the room-temperature fits of the spectra of ZnPc(−2) because the MCD spectrum is clearly dominated by the distinctive derivative-shaped *A* terms.[6] When *A* terms dominate the MCD spectrum, the band assignment is straightforward even in the presence of solvent-induced band broadening. In the case of $[ZnPc(-3)]^-$, however, both the ground and excited states are nondegenerate and the spectrum must be deconvoluted entirely with Gaussian-shaped *B* terms. The absence of the derivative-shaped *A* terms observed in the MCD spectrum of neutral and cationic MPc's makes the deconvolution analysis more difficult in the case of $[ZnPc(-3)]^-$. When both spectra are dominated by overlapping Gaussian bands, meaningful band-fitting can only be carried out if the bandwidths of the absorption and MCD spectra are *identical* in value, as assumed under the rigid-shift approximation.

Table 2. Band Centers (nm) in the Optical Spectra of $[ZnPc(-3)]^-$

77 K abs	room-temp MCD	room-temp abs	77 K abs	room-temp MCD	room-temp abs
957	957	962	571	566	570
930	928		430	429	428
878	881	875		377	
791	792	796	321	313	324
634	630	638			

In the case of $[ZnPc(-3)]^-$ the MCD bands measured at 560, 640, and 960 nm in solution at room temperature are clearly sharper than the corresponding absorption bands (Figures 4 and 5). The presence of a number of transitions under each band complicates the analysis of the $[ZnPc(-3)]^-$ spectra measured at room temperature. These "hot" bands arise from the same multitude of solvation environments that cause the bandwidth spreading in ZnPc(−2) (Figure 8). It can be seen in Figures 3 and 4 that there are only relatively minor changes in both the ZnPc(−2) and $[ZnPc(-3)]^-$ spectra on cooling solutions from 298 to 220 K. There are also only minor changes in the spectra recorded on glasses between 130 and 77 K, possibly due to the population of vibrational levels associated with the Jahn–Teller-split ground state. Below 80 K the absorption temperature does not change. The major spectral change takes place as the phase changes from solution to glass. On vitrification, the higher energy solvation environments are frozen out, resulting in significant band sharpening. In the spectra of $[ZnPc(-3)]^-$ measured at room temperature, the band centers of the negative *B* terms at 961 and 634 nm lie significantly to the blue of the corresponding

(54) Sutherland, J. C. In *The Porphyrins*; Dolphin, D., Ed.; Academic Press: New York, 1978; Vol. III, Part A, pp 225–248.

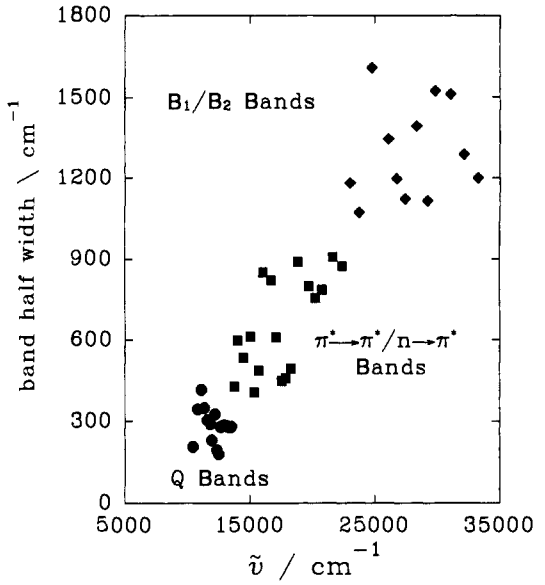

Figure 10. Scatter plot of the bandwidths used in the absorption band fit shown in Figure 9 as a function of the energy of the band center. The symbols indicate bandwidths taken from the following regions of the spectrum: (circles) Q band near 960 nm; (squares) $\pi^* \rightarrow \pi^*$ and $n \rightarrow \pi^*$ bands near 640 nm; (diamonds) B1/B2 bands near 380 nm.

absorption bands at 963 and 639 nm (Figure 3). At cryogenic temperatures both the absorption and MCD band maxima align as the higher energy solvation environments are frozen out during the quenching process (Table 2). It therefore seems reasonable to assume that a meaningful band deconvolution analysis can be possible made under the rigid-shift approximation on data recorded below 80 K.

Figure 9 summarizes a remarkable calculation: the complete deconvolution of the absorption spectrum of $[ZnPc(-3)]^-$ from 1000 to 280 nm. All the bands in the absorption spectrum measured at 77 K are accounted for by an associated band in the MCD spectrum measured at 40 K. As is evident from Figure 9, the absorption and MCD spectra measured from vitrified samples align closely and confirm that only a single transition is located under each major band observed at room temperature. With such a wide-energy range fit, we can make use of trends in the spectrum not normally accessible to us. Figure 10 compares the bandwidths calculated in the fit with the band maxima energy: clearly an almost linear dependence is observed. Hochstrasser and Marzzacco[49] have described how the bandwidths of similar excited states will tend to broaden for each successive state up the manifold of singlet $\pi \rightarrow \pi^*$ and of $n \rightarrow \pi^*$ excited states of aromatic and heteroaromatic molecules. The bandwidths of transitions to the higher states will be broadened due to energy uncertainty deriving from their natural radiative lifetimes. The extremely wide range of data available for use in Figure 10 allows us to suggest that there are three, or possibly four, distinct sets of bands in the optical spectrum, in the regions 300–480, 480–750, and 750–1000 nm. We believe that Figure 10 represents the first report of the effect described by Hochstrasser and Marzzacco over such a wide range of transition energies in any porphyrin or phthalocyanine. The band groupings shown in Figure 10 can be associated with different transitions of the phthalocyanine ring, and this will form the basis of our band assignments.

Band Assignments. The MCD spectrum of $[ZnPc(-3)]^-$ shown in Figure 3 contains a new class of spectral features for the phthalocyanine molecules. The three sets of coupled –/+ MCD bands in the 940-, 600-, and 400-nm regions are *characteristic markers for ring reduction.* Under C_{2v} symmetry, the Q, B1, B2, and $\pi^* \rightarrow \pi^*$ set of transitions shown in Figure 8 are all allowed. As there is a complete lifting of the orbital degeneracies in the π-system, separate bands of x- and y-polarization will arise from

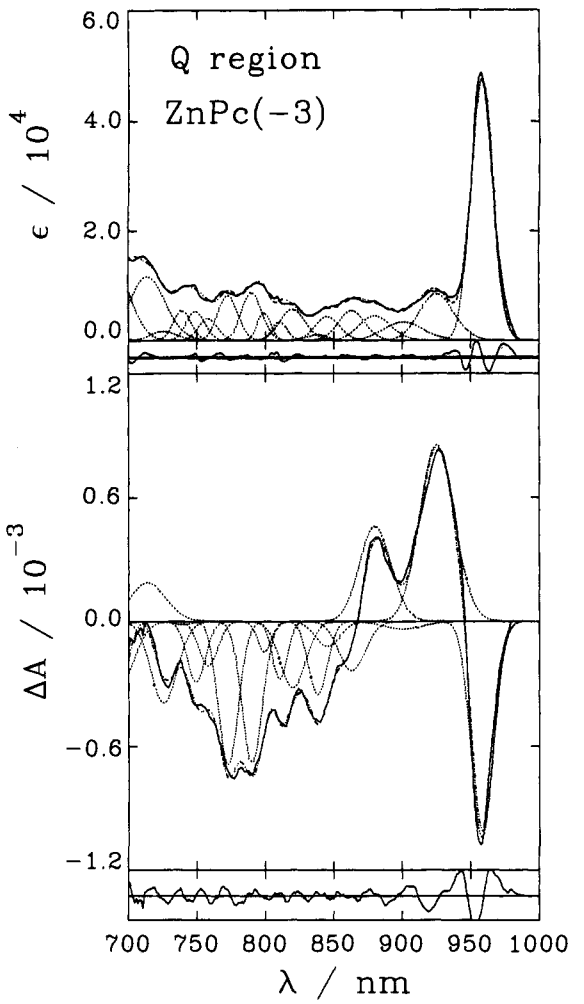

Figure 11. Complete Gaussian band fit of the absorption and MCD spectra of $[ZnPc(-3)]^-$ in the $\pi \rightarrow \pi^*$ Q band region centered on 960 nm. The absorption spectrum was recorded at 77 K, and the MCD spectrum, at 40 K. The fits were constrained by using identical band centers and bandwidths; 19 bands were required. The parameters used are summarized in Table 3.

each transition (Figure 8). In the case of ZnPc(–2) there is considerable configurational interaction between the B1 and B2 excited states.[21] The Q, B1, B2, and $\pi^* \rightarrow \pi^*$ transitions can therefore all be viewed as being essentially fully allowed, $\Delta M_L = \pm 1$, transitions. As the pairs of orbitals that would be degenerate in an ideal cyclic polyene still lie reasonably close in energy, transitions into these orbitals will mix under the influence of the applied magnetic field to give rise to pairs of intense oppositely signed B terms in the MCD spectrum. It makes sense, therefore, to continue to use the band terminology developed for MP(–2) and MPc(–2) complexes, despite the fact that each transition will now give rise to multiple excited states.

Although the electric dipole polarizations of the individual bands can be estimated through group theory, the signs observed for the MCD B terms require considerable extra calculation because good values for the angular momentum for each state must be known.[23b] As a result, a specific MCD sign cannot be related to the geometric x- or y-polarizations. A further effect of C_{2v} symmetry is to allow transitions from all four aza nitrogen nonbonding orbitals into the $M_L = \pm 5$ π^* orbitals with a combination of z- ($b_1 \rightarrow b_1$, $b_2 \rightarrow b_2$) and x- and y-polarizations ($a_1 \rightarrow b_1$, b_2) (Figure 8). The poorer orbital overlap of the ground and excited states will significantly reduce the intensity of these bands relative to the $\pi^* \rightarrow \pi^*$ and $\pi \rightarrow \pi^*$ bands. Under C_{2v} symmetry, transitions from $M_L = \pm 5$ to $M_L = \pm 7$ and from $M_L = \pm 3$ to $M_L = \pm 5$ will be allowed with z-polarization. As these

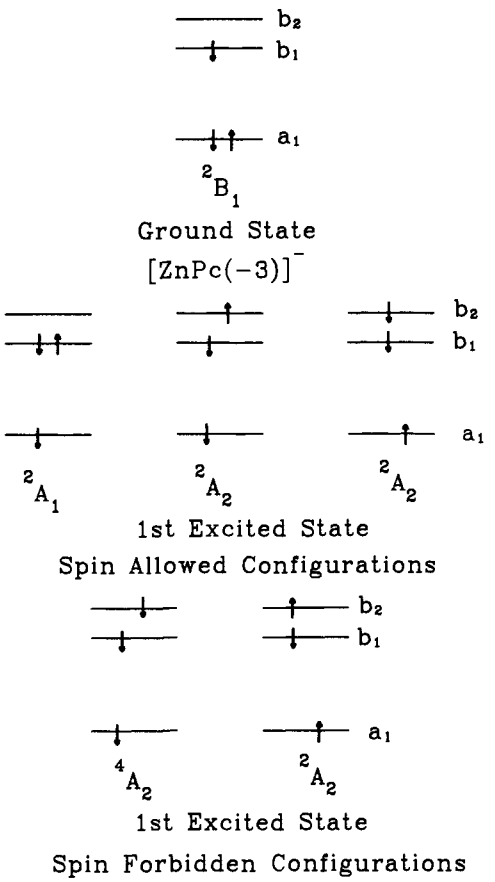

Figure 12. Electronic configurations for the ground state and first excited state. The model assumes that the e_g^* orbital splits to b_2 and b_1 in C_{4v} symmetry under the influence of Jahn–Teller and environmental distortion following reduction of the ring. Transitions to the lowest energy orbital ($a_1 \rightarrow b_2$) will result in a negative MCD signal, whereas the two $a_1 \rightarrow b_1$ transitions will result in a positive MCD signal due to coupling directly to the $a_1 \rightarrow b_2$ transition.

z-polarized transitions involve $\Delta M_L = \pm 2$, they are not fully allowed and will therefore give rise to relatively weak bands. The Q, B1, B2, and $\pi^* \rightarrow \pi^*$ sets of transitions must therefore be responsible for the major bands seen in the MCD spectrum.

The three distinct sets of bands identified by the deconvolution analysis in Figure 10 at 958/925, 635/569, and 434/383 nm represent a useful starting point for the assignments. The MCD spectra of both $[MgPc(-3)]^-$ [13] and $[ZnPc(-3)]^-$ are dominated by *B* terms, transitions that must gain the significant intensity observed by field-induced mixing between related pairs of states.[23,24] We need to associate the observed bands with transitions to the states commonly referred to as Q, B_1, and B_2 and add in the $\pi^* \rightarrow \pi^*$ bands under C_{2v} symmetry. The bands centered on 962 and 428 nm exhibit an inequivalence in the band intensities of the −/+ pairs that we interpret as an indication that these transitions involve an electron going *into* a partially filled orbital. We therefore assign these bands to the Q and B1/B2 transitions, respectively. On the other hand, the equivalence in *B* term intensities in the 600-nm pair is consistent with field-induced mixing between transitions to a pair of closely lying empty orbitals. We assign this set of bands as the allowed $\pi^* \rightarrow \pi^*$ transition out of the split e_g^* $M_L = \pm 5$ π^* orbital into the b_1^*/b_2^* $M_L = \pm 6$ π^* orbitals, as shown in Figure 8.

(1) The Q Band Region 750–1000 nm. The MCD signal in the 750–1050-nm region cannot be interpreted in terms of a simple pair of oppositely signed bands of similar intensity; see Figure 11. The initial sharp negative band is followed by two broader positive bands at room temperature. The presence of an electron in the zero-field orbitally split HOMO e_g^* orbital leads to a more complex situation than is seen in the 570/635-nm $\pi^* \rightarrow \pi^*$ region.

Table 3. Band Parameters[a] for $[ZnPc(-3)]^-$ from a Spectral Deconvolution Calculation Using SIMPFIT[30,31]

no.	ν	λ	Γ	ϵ	$\langle\epsilon\rangle_0$	D_0	$10^6\langle\Delta A\rangle_0$
1	**10 437**	**958**	**205**	**42 310**	**993.7**	**3.04**	**−21.99**
2	**10 809**	**925**	**344**	**8 440**	286.5	0.88	28.92
3	11 097	901	416	3 330	133.1	0.41	−1.34
4	**11 363**	**880**	**350**	**4 490**	**147.3**	**0.45**	**14.90**
5	11 587	863	305	5 430	152.4	0.47	−6.56
6	11 831	845	290	4 340	113.7	0.35	−3.16
7	11 932	838	229	1 010	20.7	0.06	−7.20
8	12 198	819	325	5 710	162.1	0.50	−9.01
9	12 342	810	194	3 390	56.9	0.17	−4.64
10	12 516	799	180	5 020	77.0	0.24	−2.21
11	12 658	790	280	8 710	205.0	0.62	−15.96
12	12 944	772	286	8 170	192.1	0.59	−16.26
13	13 192	758	282	3 970	90.4	0.28	−4.90
14	13 347	749	280	5 320	118.9	0.36	−6.45
15	13 526	739	280	5 450	120.0	0.37	−0.33
16	13 780	725	428	1 690	55.8	0.17	−12.88
17	14 007	713	598	11 650	530.0	1.62	8.35
18	14 454	691	535	12 090	476.2	1.45	−13.17
Q_{00}	14 862	672	280	4 420	88.7		−8.34
19	15 031	665	612	24 600	1066.9	3.27	−28.19
20	15 343	651	408	40 420	1145.1	3.51	23.99
21	**15 725**	**635**	**488**	**73 220**	**2420.8**	**7.41**	**−211.60**
22	16 064	622	851	27 860	1571.1	4.81	−87.39
23	16 740	597	821	28 780	1506.0	4.61	56.68
24	17 112	584	610	49 760	1899.4	5.82	101.67
25	**17 552**	**569**	**449**	**59 420**	**1622.4**	**4.97**	**152.26**
26	17 881	559	460	36 750	1007.6	3.09	23.41
27	18 297	546	495	23 710	684.9	2.10	7.54
28	18 853	530	890	22 090	1110.2	3.40	2.98
29	19 736	506	798	7 360	317.3	0.97	−0.52
30	20 248	493	756	2 270	90.3	2.31	0.38
31	20 800	480	786	3 100	125.0	0.38	−0.52
32	21 670	461	907	5 650	252.0	0.77	1.66
33	22 403	446	873	1 770	73.7	0.23	3.93
34	**23 031**	**434**	**1181**	**40 970**	**2237.2**	**6.85**	**−67.51**
35	23 900	420	1072	11 000	527.7	1.62	−13.69
36	**24 779**	**403**	**1608**	**28 600**	**1975.9**	**6.05**	**−46.34**
37	**26 088**	**383**	**1347**	**26 940**	**1481.0**	**4.53**	**54.73**
38	26 755	373	1196	19 850	946.1	2.90	2.57
39	**27 431**	**364**	**1122**	**25 600**	**1117.5**	**3.42**	**14.54**
40	28 384	352	1394	42 950	2246.6	6.88	9.96
41	29 247	341	1115	11 500	466.9	1.43	−1.52
42	**29 879**	**334**	**1523**	**38 240**	**2079.8**	**6.37**	**5.11**
43	**31 078**	**321**	**1509**	**44 970**	**2328.0**	**7.13**	**8.14**
44	32 159	310	1289	38 460	1641.4	5.03	1.46
45	33 270	300	1199	34 770	1342.6	4.11	−0.28

[a] Key: no., band number from low to high energy (Q_{00} refers to the ZnPc(−2) Q band); ν, calculated energy of the band center in wavenumbers; λ, wavelength of the band center in nanometers; Γ, bandwidth in wavenumbers; ϵ, extinction coefficient at the band center in units of $cm^{-1}\cdot mol^{-1}\cdot L$; $\langle\epsilon\rangle_0$, zeroth moment of the absorption band intensity; D_0, calculated dipole strength, $D_0 = \langle\epsilon\rangle_0/326.6$, in units of D^2 (D = Debye units);[24a] $\langle\Delta A\rangle_0$, zeroth moment of the MCD band intensity. The bold type indicates energies of the major electronic transitions.

The negative 957-nm *B* term arises from a transition into the lower partially filled orbital (Figure 8). The presence of the electron in the lower orbital means that there are two separate allowed excited-state configurations where an electron goes into the higher unfilled orbital (Figure 12). These configurations will interact with each other and could result in the two separate positive *B* terms seen to the blue of the initial intense negative *B* term. The fit for this region is shown as Figure 12, with the parameters given in Table 3. We see in Figure 11 that there are a large number of bands that make up the trailing blue edge to the Q_{00} transition. The nature of this series of bands suggests that there are at least two or three vibronic progressions based on the *x*- and *y*-components of the Q band. It should be noted that similar MCD spectra have been reported for chlorophylls where there is also a lifting of ground- and excited-state degeneracies.[55]

(2) The $\pi^* \rightarrow \pi^*$ Band Region 500–750 nm. The $\pi^* \rightarrow \pi^*$ transition is assigned to the "pseudo" *A* terms which dominates

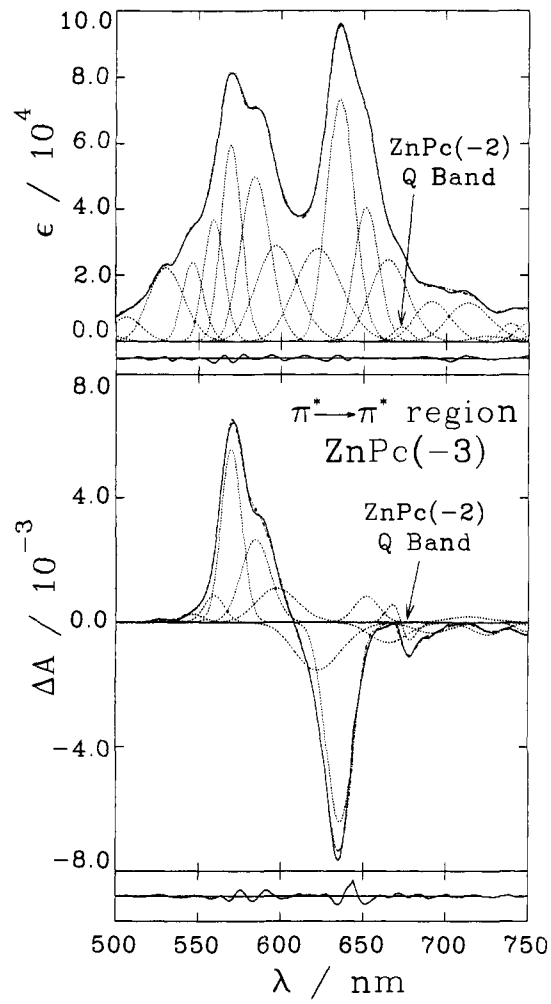

Figure 13. Complete Gaussian band fit of the absorption and MCD spectra of $[ZnPc(-3)]^-$ in the $\pi^* \rightarrow \pi^*$ band region centered on 640 nm. The absorption spectrum was recorded at 77 K, and the MCD spectrum, at 40 K. The fits were constrained by using identical band centers and bandwidths; 19 bands were required. The parameters used are summarized in Table 3.

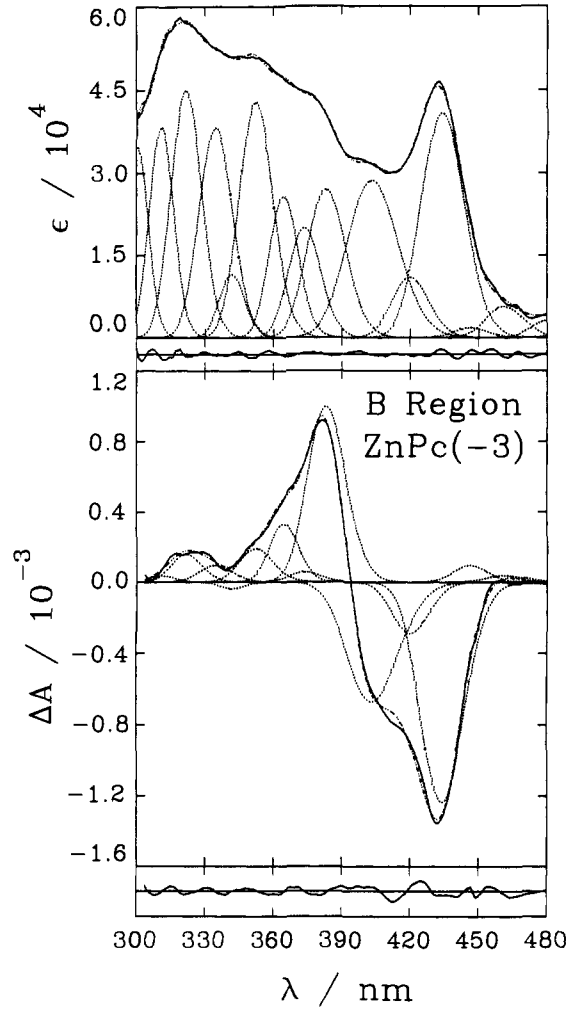

Figure 14. Complete Gaussian band fit of the absorption and MCD spectra of $[ZnPc(-3)]^-$ in the $\pi \rightarrow \pi^*$ B1/B2 band region centered on 425 nm. The absorption spectrum was recorded at 77 K, and the MCD spectrum, at 40 K. The fits were constrained by using identical band centers and bandwidths; 15 bands were required. The parameters used are summarized in Table 3.

the MCD spectrum at 569 and 635 nm; see Figure 13. These bands arise from a transition linking an orbitally nondegenerate ground state with two excited states associated with the empty a_1^* and a_2^* orbitals which would be degenerate if the ring was an ideal cyclic polyene. It can be seen that the spectral bands in the 640–750-nm region are significantly broader than the bands associated with the Q transition (Figures 9 and 10). These bands cannot be associated with the $\pi^* \rightarrow \pi^*$ transition, as they lie to the low-energy side of the "pseudo" *A* term. As these broad bands are over 3000 cm^{-1} from the initial negative *B* term of the Q transition, it seems unlikely that they are vibrational in origin. We therefore tentatively assign these bands to transitions linking the lone-pair orbitals on the aza nitrogens and the HOMO Jahn–Teller-split e_g^* level of $[ZnPc(-3)]^-$. Bearing in mind the findings of Hochstrasser and Marzzacco,[49] this could in part account for the significant broadening of the bands in the B1/B2 region. The bands to the blue of the 569-nm band are very weak in the MCD spectrum relative to the absorption spectrum; see Table 3. These bands can be assigned primarily to vibrational bands associated with the $\pi^* \rightarrow \pi^*$ transition. The three bands between 569 and 635 nm are more difficult to explain in simple terms. The overlap of the $\pi^* \rightarrow \pi^*$ bands with bands associated with $n \rightarrow \pi^*$ transitions could certainly lead to the highly complex set of bands that is seen in this region of the optical spectrum of $[ZnPc(-3)]^-$.

(3) The B1/B2 Band Region 300–480 nm. In the B band region the MCD signal is similar to that seen in the Q region, but there is significantly greater absorption intensity to the blue of the intense negative 434-nm *B* term. The deconvolution shown in Figure 14 shows that the structure of the optical spectrum in this region is much more complex. The most likely explanation is that there are in fact two overlapping transitions present which correspond to the B1 and B2 transitions of ZnPc(−2); see Figures 7 and 8. These transitions will result in sets of excited-state configurations that are similar to that seen with the Q transition (Figure 12). The bands at 434, 383, and 334 nm in Figure 14 are assigned to the B1 transition, and the bands at 403, 364, and 321 nm are assigned to the B2 transition. Hydrazine hydrate has an intense absorption band at 280 nm, and the solvent cutoff of DMF is at about 260 nm. As a result, the vibrational bands to the blue of the initial B1/B2 transitions are not seen. Configurational interaction between the excited states associated with these two transitions has been predicted to be particularly significant.[21] This accounts for the far larger energy separations seen between the initial negative and positive MCD bands in the B1/B2 region compared to the Q region of the spectrum (Figure 9). In the absence of configurational interaction, the separation between these band would closely reflect the energy separation

(55) (a) Briat, B.; Schooley, D. A.; Records, R.; Bunnenberg, E.; Djerassi, C. *J. Am. Chem. Soc.* **1977**, *89*, 6170. (b) Weiss, C. In *The Porphyrins*; Dolphin, D., Ed.; Academic Press: New York, 1978; Vol. III, Part A, pp 211–223. (c) Frakowiak, D.; Bauman, D.; Manikowski, H. Browett, W. R.; Stillman, M. J. *Biophys. Chem.* **1987**, *28*, 101.

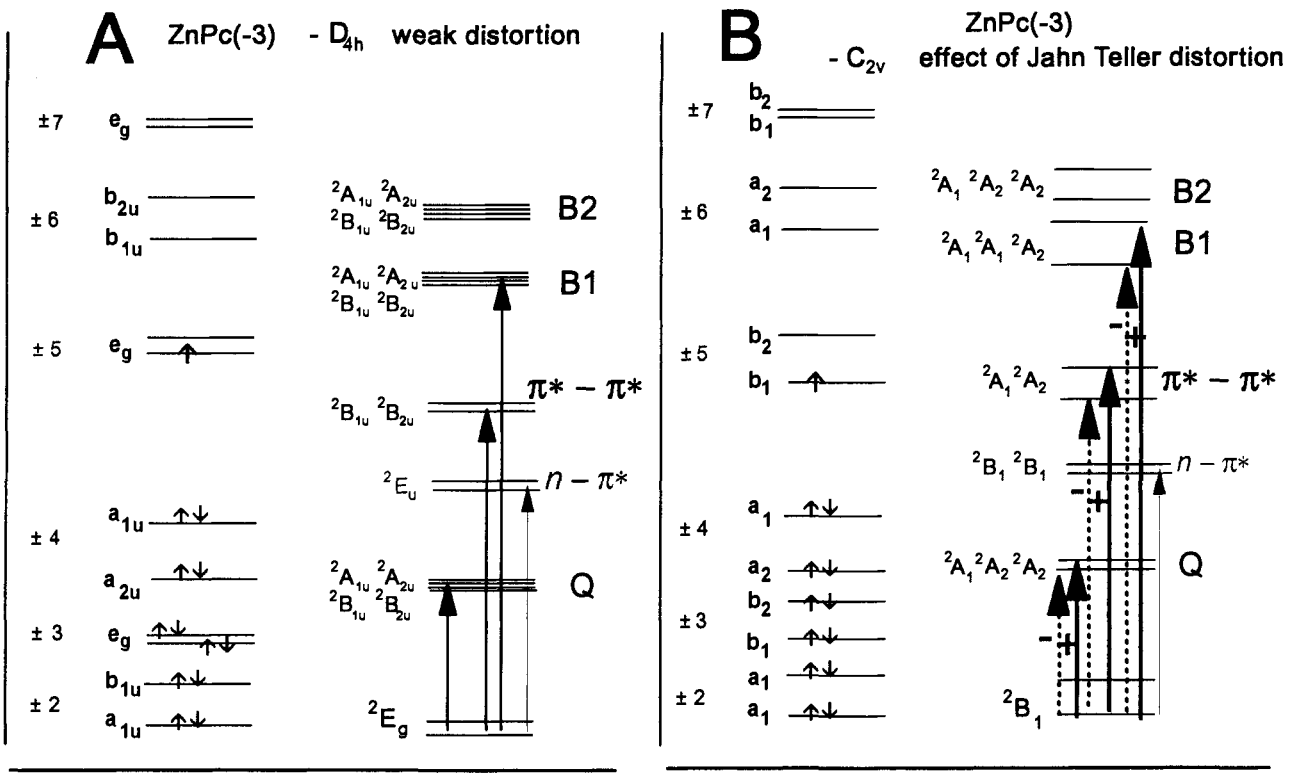

Figure 15. Energy level diagram based on the interpretation of the optical data for $[ZnPc(-3)]^-$. (A) In the absence of significant Jahn–Teller distortion, the lowest energy transitions will exhibit temperature-dependent MCD *C* terms. The states are shown with a weak static distortion where the degeneracy of the ^2E_g ground state is only partially broken. The broad arrows refer to *x*/*y*-polarized transitions, and the narrow arrow refers to a *z*-polarized transition. (B) The lack of any significant temperature dependence in the MCD spectrum is unambiguous evidence that the ground state is nondegenerate. Combination of static Jahn–Teller and environmental distortions due to solvation reduces the effective symmetry to C_{2v}. The ground-state symmetry is therefore $^2B_1$. The broad arrows show the sign of the *B* terms located under each major 0–0 band that arises from the coupled *x*- and *y*-polarized transitions. There are three spin-allowed excited states associated with the Q transition that arise from the configurations shown as Figure 12: $^2A_1$, $^2A_2$, $^2A_2$. The lowest lying n → π* transition gives rise to two $^2B_1$ excited states. Two higher lying n → π* transitions would give rise to $^2A_1$, $^2A_2$, $^2A_2$ excited states but are not shown. The π* → π* states transform as $^2A_1$, $^2A_2$. The B1 and B2 transitions give rise to states that transform as $^2A_1$, $^2A_2$, $^2A_2$ (B1) and $^2A_1$, $^2A_1$, $^2A_2$ (B2).

of the two levels of the HOMO Jahn–Teller-split e_g* level. The configurational interaction between the B1 and B2 (which may also involve the higher lying N and L) transitions will inevitably result in a far more complex set of bands than was seen in the Q region.

(4) State Level Diagrams for Anion Radical Species. MCD spectroscopy provides the ground- and excited-state degeneracy information that is required before meaningful band assignments of the optical spectra of metal phthalocyanine and porphyrin anion radical species can be made. Figure 15 compares the orbital and state level diagrams that would result from differing degrees of distortion of the ground state. If the ground state is only slightly distorted, the molecule would essentially retain D_{4h} symmetry and the MCD spectrum would show a marked temperature dependence due to the degeneracy, or near-degeneracy, of the ground state. When the splitting is more substantial, as was the case with $[ZnPc(-3)]^-$, the molecular symmetry drops to C_{2v} and there is a complete lifting of ground- and excited-state degeneracies. The resonance Raman study of Perng and Bocian on the anion radical species has shown that the anticipated degenerate ground states of $[ZnOEP(-3)]^-$ and $[ZnTPP(-3)]^-$ are orbitally split to differing extents by Jahn–Teller distortion.[22a] MCD spectroscopy would provide the perfect probe for determining quantitatively the extent of this zero-field orbital splitting. We can directly calculate the energy between the ground state and any close-lying state from the temperature dependence observed in the MCD spectrum. As we have described already, there is no significant temperature dependence in the MCD spectrum of $[ZnPc(-3)]^-$, which means that the two components must be separated by at least 800 cm^{-1} (based on a 5% occupancy at 300 K) to reduce the Boltzmann distribution to a level that results in a temperature-independent MCD signal.

Conclusion

In summary, we report the photochemical formation and extensive optical studies of the ring-reduced radical anion species $[ZnPc(-3)]^-$. Analysis of the low-temperature absorption and MCD spectral data provides a unique set of optical parameters that define the electronic configuration of the anion radical. These novel data provide definitive parameters for use in theoretical calculations for both phthalocyanines and porphyrins. The data reported here illustrate the value of experimental MCD data in providing unique polarization information for a chemically challenging species that allows assignments of the major bands in the optical spectrum to be made.

Acknowledgment. We gratefully acknowledge financial support from the Natural Sciences and Engineering Research Council of Canada (to M.J.S.) and the Province of Ontario for a Differential Fee Bursary (to J.M.). M.J.S. is a member of the Centre for Chemical Physics and the Photochemistry Unit at the University of Western Ontario and acknowledges their continued support of this work. This is publication No. 469 of the Photochemistry Unit.